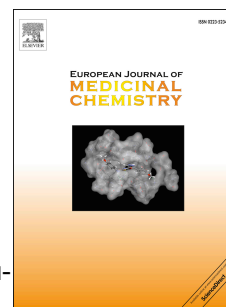


Accepted Manuscript

Combination of amino acid/dipeptide with ligustrazine-betulinic acid as antitumor agents

Bing Xu, Wen-Qiang Yan, Xin Xu, Gao-Rong Wu, Chen-Ze Zhang, Yao-Tian Han, Fu-Hao Chu, Rui Zhao, Peng-Long Wang, Hai-Min Lei



PII: S0223-5234(17)30101-0

DOI: [10.1016/j.ejmech.2017.02.036](https://doi.org/10.1016/j.ejmech.2017.02.036)

Reference: EJMECH 9232

To appear in: *European Journal of Medicinal Chemistry*

Received Date: 5 January 2017

Revised Date: 12 February 2017

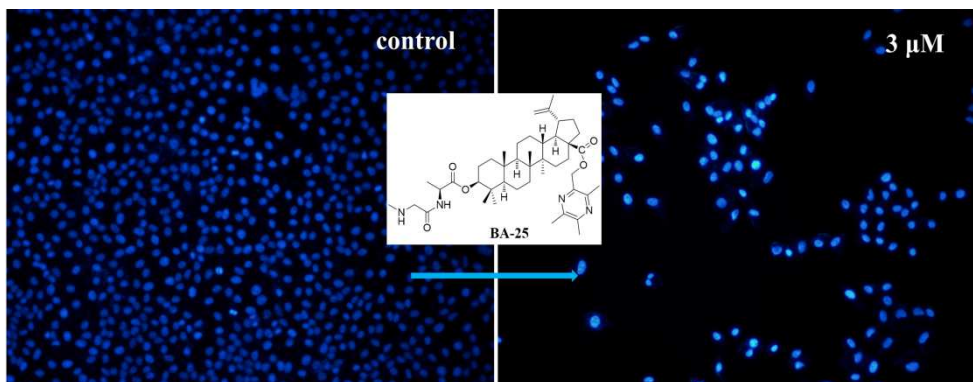
Accepted Date: 13 February 2017

Please cite this article as: B. Xu, W.-Q. Yan, X. Xu, G.-R. Wu, C.-Z. Zhang, Y.-T. Han, F.-H. Chu, R. Zhao, P.-L. Wang, H.-M. Lei, Combination of amino acid/dipeptide with ligustrazine-betulinic acid as antitumor agents, *European Journal of Medicinal Chemistry* (2017), doi: 10.1016/j.ejmech.2017.02.036.

This is a PDF file of an unedited manuscript that has been accepted for publication. As a service to our customers we are providing this early version of the manuscript. The manuscript will undergo copyediting, typesetting, and review of the resulting proof before it is published in its final form. Please note that during the production process errors may be discovered which could affect the content, and all legal disclaimers that apply to the journal pertain.

Graphical Abstract

New series of TBA amino acid/dipeptide derivatives were synthesized and evaluated for their antitumor activity. **BA-25** was found to be the most active one.



1 Original article

2 **Combination of Amino Acid/Dipeptide with** 3 **Ligustrazine-Betulinic Acid as Antitumor Agents**

4 **Bing Xu^a, Wen-Qiang Yan^a, Xin Xu^a, Gao-Rong Wu^a, Chen-Ze Zhang^a,**
5 **Yao-Tian Han^a, Fu-Hao Chu, Rui Zhao^a, Peng-Long Wang^{a,*}, Hai-Min Lei^{a,*}**

6 ^a School of Chinese Pharmacy, Beijing University of Chinese Medicine, Beijing
7 100102, China

8 *To corresponding author: e-mail address: hm_lei@126.com (H. Lei),
9 wpl581@126.com (P. Wang)

10 **Abstract:** The lead compound **TBA**, 3 β -Hydroxy-lup-20(29)-ene-28-oic acid-3,
11 5, 6-trimethylpyrazin-2-methyl ester, which exhibited promising antitumor
12 activity and induced tumor cell apoptosis in various cancer cell lines, had
13 previously been reported. Moreover, reports have revealed that the introduction
14 of amino acid to betulinic acid could improve selective cytotoxicity as well as
15 water solubility. Thus, a series of novel **TBA** amino acid and dipeptide
16 derivatives were designed, synthesized and screened for selective cytotoxic
17 activity against five cancer cell lines (HepG2, HT-29, Hela, BCG-823 and A549)
18 and the not malignant cell line MDCK by standard MTT assay. Most of the
19 tested **TBA**-amino acid and dipeptide analogues showed stronger
20 anti-proliferative activity against all tested tumor cell lines than **TBA**. Among
21 them, **BA-25** exhibited the greatest cytotoxic activity on tumor cell lines (mean
22 $IC_{50} = 2.31 \pm 0.78 \mu M$), that was twofold than the positive drug cisplatin (**DDP**),
23 while it showed lower cytotoxicity on MDCK cell line than DDP. Further cell
24 apoptosis analyses indicated **BA-25**-induced apoptosis was associated with loss
25 of mitochondrial membrane potential and increase of intracellular free Ca^{2+}
26 concentration.

27 **Keywords:** Betulinic acid, Amino acids derivatives, Dipeptide derivatives, Selective
28 cytotoxicity, Structure-activity relationships, Apoptosis;

1. Introduction

Cancer is one of the major diseases which threatens human life and health seriously [1-2]. The cytotoxic agents are still one of the main clinical treatments for the malignant tumor. However, these drugs usually have some severe side effects with poor patients compliance, therefore the discovery of the targeted anti-tumor drugs is of great significance [3-6]. Because of their strong selective cytotoxicity and potent apoptosis induction activity, pentacyclic triterpenoids and their derivatives had become the focus of scientific interest [7-10].

Ligustrazine (2,3,5,6-tetramethylpyrazine, TMP), a major effective component of traditional Chinese medicine Rhizoma Chuanxiong (*Ligusticum, chuanxiong Hort*), has been used for the treatment of cardiovascular and cerebrovascular diseases in the clinic in China for many years [11-13]. Recently, ligustrazine was found to possess anticancer activity *in vivo* and *in vitro*, it could induce cancer cell apoptosis and reverse multidrug resistance in tumors [14-16]. Meanwhile, recent researches revealed that the introduction of ligustrazine to the anti-tumor components could increase their cytotoxicity and selectivity [17, 18]. This has stimulated interest in using ligustrazine as the scaffold to synthesize new anticancer agents by combination it with other anti-tumor ingredients [16, 19-21]. In our previous study, we successfully synthesized a series of novel ligustrazine-triterpenes derivatives and observed that these derivatives possessed potent selective cytotoxicity, of which, 3 β -Hydroxy-lup-20(29)-ene-28-oic acid-3, 5, 6-trimethylpyrazin-2-methyl ester (**TBA**) displayed promising selective cytotoxicity (IC₅₀ < 5.23 μ M) [17-19, 21, 22]. In addition, reports have shown that the introduction of amino acid or dipeptide to triterpenes could improve selective cytotoxicity as well as water solubility [8, 21, 23-25]. Based on the above, we attempted the synthesis of several **TBA** amino acids and dipeptide derivatives **BA-X** by introducing various amino acids or dipeptides to the C3 of **TBA**, in order to improve its antitumor activities and tumor targeting. All newly synthesized compounds were fully characterized by ¹H-NMR, ¹³C-NMR, HRMS and tested for cytotoxic activity against a panel of tumor cell lines and normal cell line, including HepG2, HT-29, Hela, BGC823, A549 and MDCK. Meanwhile, the

preliminary anti-tumor mechanisms of the most potent compound were also investigated by fluorescence staining observation and flow cytometric analysis in present study. In addition, the structure-activity relationships of these derivatives were briefly discussed.

2. Results and discussion

2.1. Chemistry

The designed derivatives were prepared following the procedures in Scheme 1-4. The compound **TBA** (**BA-01**) was prepared according to our previous study with some modifications [19]. According to the literature procedure, the intermediate (3,5,6-trimethylpyrazin-2-yl)methanol (**4**) was successively obtained [26]. Then the intermediate **4** was further reacted with tosyl chloride (TsCl) in tetrahydrofuran (THF) in the presence of triethylamine (TEA) and 4-dimethylaminopyridine (DMAP) to yield the important intermediate 2-(chloromethyl)-3,5,6-trimethylpyrazine (**5**) (Scheme 1). Subsequently, it underwent alkylation reaction in N, N-dimethylformamide (DMF) with betulinic acid (BA) to afford the compound **TBA** (**BA-01**) (Scheme 2).

(Insert Scheme 1)

(Insert Scheme 2)

The **TBA** amino acid derivatives **BA-02**---**BA-15** (Scheme 3, Table 1) were obtained by 1-Ethyl-3-(3-dimethylaminopropyl)carbodiimide hydrochloride (EDCI) mediated esterification from the corresponding protected (N-Boc, N-Cbz) amino acids and **TBA**. Deprotection was performed with trifluoroacetic acid (TFA) in dry dichloromethane (DCM) or by treating the compounds with Pd/C (10%) in methanol (MeOH). It was worth noting that, to avoid the formation of undesirable by-products, the hydroxyl groups of Cbz-L-serine and Cbz-L-threonine should be protected with tert-Butyldimethylsilyl chloride (TBDMSCl) before esterification with **TBA** in the synthesis of **BA-14** and **BA-15**. Removal of the TBDMS groups was achieved using

86 1M tetrabutylammonium fluoride (TBAF) solution in THF (Scheme 3).

87 (Insert Scheme 3)

88 (Insert Table 1)

89 (Insert Table 1)

90 In similar fashions, the TBA dipeptide derivatives **BA-16**---**BA-27** were prepared
91 according to the procedures in Scheme 4. In brief, the TBA amino acids derivatives
92 **BA-02**, **BA-04**, **BA-06** and **BA-12** underwent peptide coupling reactions with the
93 corresponding N-Boc protected amino acids (L-Gly, L-Sar, L-Pro, L-Ala) in the
94 presence of EDCI, 1-hydroxybenzotriazole (HOBt) and N, N-Diisopropylethylamine
95 (DIPEA) in dry DCM to afford the corresponding **TBA** dipeptide intermediates,
96 which were further treated with TFA in dry DCM to give the final compounds
97 **BA-16**---**BA-27** (Table 2). The structures of all target derivatives were confirmed by
98 spectral (¹H-NMR, ¹³C-NMR and HRMS) analysis.

99 (Insert Scheme 4)

100 (Insert Table 2)

101 2.2. Biology

102 2.2.1 Cytotoxicity Assay

103 The *in vitro* antitumor activity of **TBA** amino acids and dipeptide derivatives was
104 evaluated on five tumor cell lines (HepG2, HT-29, Hela, BCG-823, A549) using the
105 standard MTT assay, and their toxicity was tested using MDCK cells. The IC₅₀ values
106 were summarized in Table 3. As shown in Table 3, after combination with amino acid
107 or dipeptide, most of the targeted compounds showed significantly improved
108 cytotoxicity on all tested tumor cell lines compared to the starting material **TBA**. The
109 cytotoxicity detection also revealed that most of **TBA** amino acids derivatives (such
110 as **BA-02**, **BA-09**, **BA-10**, **BA-12** et al) and nearly all **TBA** dipeptide derivatives
111 exhibited better antiproliferative activities than the positive drug DDP, while they
112 showed lower cytotoxicity than DDP on MDCK cell line. Among the candidates,

BA-25 was the most active one, which exhibited perfect antiproliferative activities (mean $IC_{50} = 2.31 \pm 0.78 \mu M$) on all tested cancer cell lines. For example, the IC_{50} values of **BA-25** for HT-29, Hela and BGC-823 ($1.70 \pm 0.34 \mu M$, $1.74 \pm 0.99 \mu M$, $1.79 \pm 0.28 \mu M$) is much lower than those of the positive drug cisplatin (DDP) ($4.10 \pm 1.17 \mu M$, $5.60 \pm 0.78 \mu M$, $4.25 \pm 0.32 \mu M$). Meanwhile **BA-25** exhibited higher cytotoxic selective towards MDCK cells ($IC_{50} = 10.84 \pm 0.27 \mu M$) than DDP. It is worth noting that, although the compound **BA-10**, **BA-23** and **BA-24** exhibited slightly lower cytotoxicity than **BA-25** on the tested cancer cells, their pronounced cytotoxic selective (therapeutic index (TI) > 10) towards MDCK cells distinguished them from this series. Their IC_{50} value for MDCK cells was more than 40 μM (see Table 3).

From the obtained results, it was observed that **TBA** aliphatic amino acids derivatives exhibited better anti-proliferative activities than those aromatic amino acids and heterocyclic amino acids derivatives, as exemplified by **BA-02**, **BH-04**, **BA-10**, **BA-12** > **BA-03**, **BA-11**; Structure-activity relationship analysis among the **TBA** aliphatic amino acids derivatives also revealed that the compounds with small molecule aliphatic amino acids seemed to be more active than those with high molecular weight aliphatic amino acids, such as **BA-02**, **BA-04** > **BA-07**, **BA-08**. In addition, it was observed the **TBA** basic amino acids derivatives seemed to be more active than those acidic amino acids derivatives, such as **BA-10** > **BA-05**. The result also revealed that the **TBA** dipeptide derivatives were more active than the amino acids derivatives. Potency is an important criterion for assessing leads, but it is not the only consideration when selecting a lead compound for further optimization into a drug [27, 28]. The selectivity, solubility and hydrophobicity were also essential to the perfect drug candidates, because these properties were closely associated with absorption, distribution, metabolism, excretion and toxicity (ADMET) properties of the compounds [29-31]. Thus the compound **BA-10**, **BA-23**, **BA-24** and **BA-25** was selected for further pharmacodynamics and pharmacokinetic evaluation, including the *in vivo* antitumor activity and plasma stability, *in vivo* pharmacokinetics, in the hope of producing drug candidates for drug development. And the results will be reported in due course. Meanwhile the most active compound **BA-25** (mean $IC_{50} = 2.31 \pm 0.78 \mu M$) was selected for further analysis to study its mechanism of growth inhibition on HepG2 cell line in this study.

146 (Insert Table 3.)

147 2.2.2. Analyses of apoptosis

148 2.2.2.1. Morphological detection of apoptosis using Giemsa staining

149 To investigate the mechanism of HepG2 cell death induced by **BA-25**, the
150 morphologic changes of cells were observed by Giemsa staining. As shown in Fig. 1,
151 the morphology of HepG2 cells in the negative control was normal; When the cells
152 treated with **BA-25** (1.5, 3, 6 μ M) for 72 h, typical signs for apoptosis were found.
153 Even at low concentration of **BA-25** (1.5 μ M), cells had showed typical apoptosis
154 morphological features, such as cell shrinkage, chromatin margination and nuclear
155 fragmentation. With the increase of the concentration of **BA-25**, the characteristic of
156 apoptosis was more and more obvious. When the concentration of **BA-25** was raised
157 up to 6 μ M, almost all cells showed typical apoptotic morphological changes such as
158 nuclear condense, nuclear fragmentation. These results indicated that **BA-25**
159 significantly induced HepG2 cells apoptosis.

160 (Insert Fig. 1)

161 2.2.2.2. Morphological detection of apoptosis using DAPI staining

162 To further characterize the effects of apoptosis induction of **BA-25** on HepG2, the
163 nucleus morphological changes in **BA-25**-treated HepG2 were observed by DAPI
164 staining. After **BA-25** treatment for 72 h, HepG2 cells showed nuclear morphological
165 changes typical of apoptosis in a dose-dependent manner, such as nuclear
166 condensation, nuclear fragmentation and the formation of apoptotic bodies (Fig. 2).

167 (Insert Fig. 2)

168 2.2.2.3. Detection of apoptosis using Annexin V-FITC/PI staining

169 To further perform a comprehensive view on the apoptosis induced by **BA-25**,
170 apoptotic rates were analyzed by flow cytometry using an Annexin V-FITC/PI
171 staining. As shown in Fig. 3, the HepG2 cells demonstrated a remarkable response to
172 the apoptotic effect of **BA-25** in a dose-dependent fashion. The apoptotic effect was
173 determined by counting the apoptosis ratios (including the early and late apoptosis
174 ratios). Following different concentrations (2, 3, 4 μ M) of **BA-25** treatment, the
175 apoptosis ratios increased from 6.3% of the control to 10.9%, 17.8%, 36.8%,

respectively. These results indicated that **BA-25** had the potential to induce HepG2 cell apoptosis.

(Insert Fig. 3)

2.2.2.4. Measurement of mitochondrial membrane potential

Disruption of mitochondrial membrane potential ($\Delta\Psi_m$) is one of the earliest intracellular events that occur following the onset of apoptosis [32, 33]. To study whether the mitochondrial events were involved in the apoptosis induced by **BA-25**, $\Delta\Psi_m$ was measured quantitatively using flow cytometry with cell-permeable cationic dye Rhodamine 123 (Rh123). Rh123 accumulates in normal mitochondria due to its high negative charge, and the reduction of $\Delta\Psi_m$ will lead to the release of Rh123 and reduction of its fluorescence intensity [34]. As shown in Fig. 4, the fluorescent intensity decreased in a dose-dependent manner. HepG2 cells treated with **BA-25** (2 μ M, 3 μ M, 4 μ M) for 72 h exhibited a lower fluorescent intensity (MFI: 6416, 5411, 2147) compared with untreated HepG2 cells (MFI: 26410) (Fig. 4).

(Insert Fig. 4)

2.2.2.5. Assessment of intracellular Free Ca^{2+}

A sustained increase in intracellular Ca^{2+} concentrations is recognized as a factor for cell death or injury [35]. The membrane-permeable Ca^{2+} -sensitive fluorescent dye Fluo-3AM was used to evaluate the level change of intracellular free Ca^{2+} in HepG2 cell line after co-culture with **BA-25**. The Fluo-3 AM can across the cell membrane and be cut into Fluo-3 with the cells. The Fluo-3 can specifically combine with the Ca^{2+} and has a strong fluorescence with an excitation wavelength of 488 nm [36, 37]. As shown in Fig. 5, with the increase of **BA-25** concentration, intracellular free Ca^{2+} fluorescence increased dramatically (MFI 2743, 3760, 6353) compared with the control group (MFI 1992). The results indicated that the increase of intracellular Ca^{2+} was related with **BA-25**-induced HepG2 cell apoptosis (Insert Fig. 5).

3. Conclusions

In this study, we successfully synthesized 27 novel **TBA** amino acid and dipeptide derivatives by attaching different amino acids or dipeptides to the C3 of **TBA**. Their cytotoxicity was determined by the standard MTT assay. The result indicated that

most of the synthesized **TBA**-amino acid and dipeptide analogues showed significantly improved selective cytotoxicity against all tested tumor cell lines compared to **TBA**. From the obtained result, we also observed that the compounds with small molecule aliphatic amino acids seemed to be more active than those with high molecular weight aliphatic amino acids, such as **BA-02**, **BA-04** > **BA-07**, **BA-08**; The **TBA** dipeptide derivatives were more active than the amino acids derivatives. Among all the new derivatives, compound **BA-25** showed the greatest cytotoxicity on tumor cell lines ($IC_{50} = 2.31 \pm 0.78 \mu M$), that was twofold than the positive drug DDP, while it showed lower cytotoxicity on MDCK cell line than DDP. Further anti-tumor mechanistic investigation showed that **BA-25**-induced apoptosis in HepG2 cells was involved loss of the mitochondria membrane potential and increase of intracellular free Ca^{2+} concentration. In addition, although the compound **BA-10**, **BA-23** and **BA-24** exhibited slightly lower cytotoxicity than **BA-25** on the tested cancer cells, their pronounced cytotoxic selective towards MDCK cells distinguished them from this series. And the compound **BA-10**, **BA-23**, **BA-24** and **BA-25** was selected for further pharmacodynamics and pharmacokinetic evaluation, including the *in vivo* antitumor activity and plasma stability, *in vivo* pharmacokinetics, in the hope of producing drug candidates for drug development. These results suggested that the attempt to discover high selectivity anti-tumor lead compounds by introduction of amino acid or oligopeptides to cytotoxic agents was viable.

4. Experimental Section

4.1. Chemistry

Reagents were bought from commercial suppliers without any further purification. Melting points were measured at a rate of 5 °C/min using an X-5 micro melting point apparatus (Beijing, China) and were not corrected. Reactions were monitored by TLC using silica gel coated aluminum sheets (Qingdao Haiyang Chemical Co., Qingdao, China). The specific rotation was measured using an Autopol I (Rudolph Instruments) automatic polarimeter at 25 °C in MeOH. NMR spectra were recorded on a BRUKER AVANCE 500 NMR spectrometer (Fällanden, Switzerland) with tetramethylsilane (TMS) as an internal standard; chemical shifts δ were given in ppm and coupling

constants J in Hz. HR-MS were acquired using a Thermo Scientific TM LTQ Orbitrap XL hybrid FTMS instrument (Thermo Technologies, New York, NY, USA). Cellular morphologies were observed using an inverted fluorescence microscope (Olympus IX71, Tokyo, Japan).

(3,5,6-trimethylpyrazin-2-yl)methanol (**4**). Compound **4** was prepared according to the method described by Deng et al. [26].

2-(chloromethyl)-3,5,6-trimethylpyrazine (**5**). To a solution of the important intermediate (3,5,6-trimethylpyrazin-2-yl)methanol (**4**) (10mmol) in dry tetrahydrofuran (20 mL), TsCl (13mmol), TEA (20mmol) and DMAP (2mmol) were added. The mixture was allowed to stir at room temperature for 12 h. Then the solution was evaporated under vacuum and washed with brine. After drying the organic layer over anhydrous Na_2SO_4 and evaporating the solvent under vacuum, the crude product was purified by flash chromatography (silica gel, petroleum ether: acetone = 10:1).

3 β -Hydroxy-lup-20(29)-ene-28-oic acid-3,5,6-trimethylpyrazin-2-methyl ester (TBA). Compound **5** (5.0 mmol) and betulinic acid (5.0 mmol) were dissolved in 25 mL dry DMF, then K_2CO_3 (5.0 mmol) was added and the mixture was at 25 °C for 12 h. Then the reaction mixture was poured into ice-water and the crude product was extracted with ethyl acetate. After drying the organic layer over anhydrous Na_2SO_4 and evaporating the solvent under vacuum, the crude product was purified by flash chromatography (silica gel, petroleum ether: acetone = 10:1). White powder, yield 54.1%, mp: 184.6–185.4 °C, $[\alpha]_{\text{D}} = +16$ (c 0.50, MeOH); $^1\text{H-NMR}$ (CDCl_3) (ppm): 0.78, 0.80, 0.82, 0.96, 0.98, 1.67 (s, 3H, 30- CH_3 of BA), 2.51 (s, 3H, - CH_3), 2.53 (s, 3H, - CH_3), 2.57 (s, 3H, - CH_3), 3.02 (m, 1H), 3.19(m, 1H), 4.61, 4.74 (each, brs, 1H, = CH_2), 5.20, 5.23 (each, d, $J = 12.5$ Hz, 1H, - CH_2); $^{13}\text{C-NMR}$ (CDCl_3) (ppm): 14.7, 15.4, 15.9, 16.1, 18.3, 19.4, 20.4 (- CH_3), 20.9, 21.4 (- CH_3), 21.6 (- CH_3), 25.5, 27.4, 28.0, 29.7, 30.6, 32.1, 34.4, 36.9, 37.2, 38.1, 38.7, 38.9, 40.7, 42.4, 46.9, 49.5, 50.6, 55.4, 56.7, 64.3 (- CH_2), 79.0, 109.6, 145.4, 148.7, 148.9, 150.5, 150.9, 175.5 (- COO-); HRMS (ESI) m/z : 591.45212 $[\text{M} + \text{H}]^+$, calcd. for $\text{C}_{38}\text{H}_{58}\text{N}_2\text{O}_3$ 590.44474.

4.1.1. General Procedure for the Preparation of TBA amino acids derivatives
BA-02---BA-13

4.1.1.1. General procedure for esterification at carbon C3 (method A)

The compound **TBA** (1 equiv.) was dissolved in dry DCM (25 mL), DMAP (0.1 equiv.) and the protected amino acid (1.3 equiv.) were added. After addition of EDCI (1.5 equiv.), the mixture was stirred at 25 °C for 12 h. The reaction mixture was diluted with 50 mL CH₂Cl₂, then successively washed with water and brine (10 mL each), dried over sodium sulphate and filtered, and the solvent was evaporated. Then the crude product was purified by flash chromatography (silica gel, dichloromethane: methanol = 40:1).

4.1.1.2. General procedure for deprotection (method B)

To a solution of the Boc-protected compound in dry DCM (10 mL), TFA (1 mL/10 mL DCM) was added. The mixture was allowed to stir in ice bath for 2 h. After completion of the reaction (as monitored by TLC), the solution was evaporated and washed with a saturated sodium carbonate solution (20 mL). The aqueous layer was extracted with DCM (3 × 25 mL), the combined organic extracts were washed with brine (20 mL), dried over sodium sulfate, filtrated and evaporated. Purification was performed by flash chromatography (silica gel, dichloromethane: methanol = 40:1).

4.1.1.3. General procedure for the deprotection (method C)

Pd/C (10%; 80 mg) was added to a solution of the Cbz-protected compound in 30 mL MeOH. The mixture was stirred at room temperature for 12 h. After completion of the reaction (as monitored by TLC), the solvent was filtered to remove Pd/C. The filtrate was concentrated in vacuum and the residue was purified by flash chromatography (silica gel, dichloromethane: methanol = 40:1).

3β-(Glycyl)-lup-20(29)-ene-28-oic acid-3,5,6-trimethylpyrazin-2-methyl ester (BA-02). Obtained from **TBA** by method A and method B as a colorless powder; Yield: 75.3%; mp: 104.7–105.4 °C, [α]_D = +22 (c 0.50, MeOH); ¹H-NMR (500 MHz, CDCl₃): δ (ppm) 0.77, 0.83, 0.93 (s, each, 3H, 3×-CH₃, methyl of BA), 0.82 (s, each, 6H, 2×-CH₃, methyl of BA), 1.67 (s, 3H, 30-CH₃ of BA), 2.48, 2.50, 2.53 (s, each, 3H, 3×-CH₃, methyl of TMP), 2.96-3.01 (m, 1H, -CCHCH₂-), 3.44-3.47 (m, 2H, -CH₂NH₂), 4.50-4.53 (m, 1H, -OCOCH-), 4.58, 4.71 (brs, each, 1H, =CH₂), 5.17, 5.20 (d, each, 1H, *J* = 15Hz, -OCH₂-); ¹³C-NMR (125 MHz, CDCl₃): δ (ppm) 14.8, 16.0, 16.3, 16.6, 18.3, 19.5, 20.6 (-CH₃), 21.0, 21.5 (-CH₃), 21.8 (-CH₃), 23.9, 25.6, 28.1,

297 30.7, 32.2, 34.4, 37.1, 37.2, 38.0, 38.2, 38.5, 40.8, 42.5 (-CH₂NH₂), 47.0, 49.6, 50.6,
 298 55.6, 56.8, 64.5 (-CH₂), 81.9 (-OCOCH-), 109.8 (-CH=C-), 145.5, 148.9, 149.0, 150.6,
 299 151.1 (-CH=C-), 173.9 (-CONH₂), 175.7 (-COO-); HRMS (ESI) m/z: 648.47040
 300 [M+H]⁺, calcd. for C₄₀H₆₁N₃O₄ 647.46621.

301 *3β-(L-Phenylalanyl)-lup-20(29)-ene-28-oic acid-3,5,6-trimethylpyrazin-2-methyl*
 302 *ester (BA-03)*. Obtained from **TBA** by method A and method C as a colorless powder;
 303 Yield: 65.3%; mp: 82.0–82.7 °C; [α]_D = +186 (c 0.50, MeOH); ¹H-NMR (500 MHz,
 304 CDCl₃): δ (ppm) 0.76, 0.77, 0.80, 0.82, 0.94 (s, each, 3H, 5×-CH₃, methyl of BA),
 305 1.67 (s, 3H, 30-CH₃ of BA), 2.48, 2.50, 2.54 (s, each, 3H, 3×-CH₃, methyl of TMP),
 306 2.82–2.86 (m, 1H, -CH₂CH-), 2.96–3.02 (m, 1H, -CCHCH₂-), 3.15–3.18 (m, 1H,
 307 -CH₂CH-), 3.72–3.76 (m, 1H, -CHNH₂), 4.49–4.52 (m, 1H, -OCOCH-), 4.59, 4.71 (brs,
 308 each, 1H, =CH₂), 5.17, 5.20 (d, each, 1H, *J* = 15Hz, -OCH₂-), 7.19–7.33 (m, 5H,
 309 -C₆H₅); ¹³C-NMR (125 MHz, CDCl₃): δ (ppm) 14.6, 15.9, 16.2, 16.6, 18.1, 19.3, 20.5
 310 (-CH₃), 20.9, 21.4 (-CH₃), 21.7 (-CH₃), 23.7, 25.5, 28.0, 29.6, 30.5, 32.0, 34.2, 36.9,
 311 37.1, 37.9, 38.1, 38.3, 40.7, 41.1, 42.4, 46.9, 49.5, 50.4, 55.4, 56.1, 56.7, 64.4 (-CH₂),
 312 81.9, 109.7 (-CH=C-), 126.8, 128.6, 129.3, 137.3, 145.3, 148.8, 150.5, 156.0
 313 (-CH=C-), 174.4, 175.5 (-COO-); HRMS (ESI) m/z: 738.51666 [M+H]⁺, calcd. for
 314 C₄₇H₆₇N₃O₄ 737.51316.

315 *3β-(L-Alanyl)-lup-20(29)-ene-28-oic acid-3,5,6-trimethylpyrazin-2-methyl ester*
 316 *(BA-04)*. Obtained from **TBA** by method A and method B as a colorless powder;
 317 Yield: 73.0%; mp: 126.3–127.2 °C, [α]_D = +20 (c 0.50, MeOH); ¹H-NMR (500 MHz,
 318 CDCl₃): δ (ppm) 0.78, 0.84, 0.93 (s, each, 3H, 3×-CH₃, methyl of BA), 0.82 (brs, 6H,
 319 2×-CH₃, methyl of BA), 1.67 (s, 3H, 30-CH₃ of BA), 2.48, 2.50, 2.53 (s, each, 3H,
 320 3×-CH₃, methyl of TMP), 2.96–3.01 (m, 1H, -CCHCH₂-), 3.45–3.55 (m, 1H, -CHNH₂),
 321 4.48–4.51 (m, 1H, -OCOCH-), 4.58, 4.71 (brs, each, 1H, =CH₂), 5.17, 5.20 (d, each,
 322 1H, *J* = 15Hz, -OCH₂-); ¹³C-NMR (125 MHz, CDCl₃): δ (ppm) 14.8, 16.0, 16.3, 16.7,
 323 18.3, 19.5, 20.6 (-CH₃), 20.8, 21.0, 21.5 (-CH₃), 21.8 (-CH₃), 23.8, 25.6, 28.1, 29.8,
 324 30.7, 31.1, 32.2, 34.4, 37.0, 37.2, 38.1, 38.2, 38.5, 40.8, 42.5, 47.0, 50.5 (-CHNH₂),
 325 50.6, 55.5, 56.8, 64.5 (-CH₂), 81.6 (-OCOCH-), 109.8 (-CH=C-), 145.5, 148.9, 149.0,

150.6, 151.1 (-CH=C-), 175.7 (-COCH-), 176.3 (-COO-); HRMS (ESI) m/z:
662.48627 [M+H]⁺, calcd. for C₄₁H₆₃N₃O₄ 661.48186.

3β-(L-Aspartyl)-lup-20(29)-ene-28-oic acid-3,5,6-trimethylpyrazin-2-methyl ester
(**BA-05**). Obtained from **TBA** by method A and method C as a colorless powder. Yield:
45.6%; mp: > 210 °C, [α]_D = +36 (c 0.50, MeOH); HRMS (ESI) m/z: 706.47534
[M+H]⁺, calcd. for C₄₂H₆₃N₃O₆ 705.47169.

3β-(L-Prolyl)-lup-20(29)-ene-28-oic acid-3,5,6-trimethylpyrazin-2-methyl ester
(**BA-06**). Obtained from **TBA** by method A and method B as a colorless powder;
Yield: 72.7%; mp: 147.4–148.3 °C, [α]_D = +13 (c 0.50, MeOH); ¹H-NMR (500 MHz,
CDCl₃): δ (ppm) 0.77, 0.83, 0.93 (s, each, 3H, 3×-CH₃, methyl of BA), 0.82 (brs, 6H,
2×-CH₃, methyl of BA), 1.67 (s, 3H, 30-CH₃ of BA), 2.48, 2.50, 2.53 (s, each, 3H,
3×-CH₃, methyl of TMP), 2.96–3.01 (m, 1H, -CCHCH₂-), 3.22–3.25 (m, 1H,
-CH₂CH₂-), 4.10–4.13 (m, 1H, -NHCHCH₂-), 4.47–4.56 (m, 1H, -OCOCH-), 4.59,
4.71 (brs, each, 1H, =CH₂), 5.17, 5.20 (d, each, 1H, J = 15Hz, -OCH₂-); ¹³C-NMR
(125 MHz, CDCl₃): δ (ppm) 14.8, 16.0, 16.3, 16.7, 18.2, 19.5, 20.6 (-CH₃), 21.0, 21.5
(-CH₃), 21.8 (-CH₃), 23.8, 24.6, 25.5, 28.2, 29.7, 29.8, 30.6, 32.1, 34.3, 37.0, 37.2,
38.2, 38.4, 40.8, 42.5, 46.4, 47.0, 49.6, 50.6, 55.5, 56.8, 59.7 (-NHCH-), 64.5 (-CH₂),
83.5 (-OCOCH-), 109.8 (-CH=C-), 145.5, 148.9, 149.0, 150.6, 151.1 (-CH=C-), 171.5
(-COCH-), 175.7 (-COO-); HRMS (ESI) m/z: 688.50122 [M+H]⁺, calcd. for
C₄₃H₆₅N₃O₄ 687.49751.

3β-(L-Leucyl)-lup-20(29)-ene-28-oic acid-3,5,6-trimethylpyrazin-2-methyl ester
(**BA-07**). Obtained from **TBA** by method A and method B as a colorless powder;
Yield: 58.4%; colorless powder; mp: 81.8–82.5 °C, [α]_D = +24 (c 0.50, MeOH);
¹H-NMR (500 MHz, CDCl₃): δ (ppm) 0.78, 0.83 (s, each, 3H, 2×-CH₃, methyl of BA),
0.84 (brs, 6H, 2×-CH₃, methyl of BA), 1.67 (s, 3H, 30-CH₃ of BA), 2.48, 2.50, 2.54 (s,
each, 3H, 3×-CH₃, methyl of TMP), 2.96–3.01 (m, 1H, -CCHCH₂-), 3.48 (brs, 1H,
-CHNH₂), 4.48–4.51 (m, 1H, -OCOCH-), 4.59, 4.71 (brs, each, 1H, =CH₂), 5.17, 5.20
(d, each, 1H, J = 15Hz, -OCH₂-); ¹³C-NMR (125 MHz, CDCl₃): δ (ppm) 14.8, 16.0,

16.3, 16.8, 18.3, 19.5, 20.6 (-CH₃), 21.0, 21.5 (-CH₃), 21.8 (-CH₃), 22.0, 23.1, 23.8, 25.0, 25.6, 28.2, 29.8, 30.7, 32.2, 34.4, 37.1, 37.2, 38.1, 38.2, 38.5, 40.8, 42.5, 47.0, 49.6, 50.6, 55.6, 56.8 (-CHNH₂), 64.5 (-CH₂), 69.1, 81.9 (-OCOCH-), 109.8 (-CH=C-), 145.5, 148.9, 149.0, 150.6, 151.1 (-CH=C-), 175.7 (-COO-); HRMS (ESI) m/z: 704.53546 [M+H]⁺, calcd. for C₄₄H₆₉N₃O₄ 703.52881.

3β-(L-Isoleucyl)-lup-20(29)-ene-28-oic acid-3,5,6-trimethylpyrazin-2-methyl ester (BA-08). Obtained from **TBA** by method A and method B as a colorless powder; Yield: 60.5%; mp: 88.6–89.4 °C, [α]_D = +27 (c 0.50, MeOH); ¹H-NMR (500 MHz, CDCl₃): δ (ppm) 0.78, 0.82 (s, each, 3H, 2×-CH₃, methyl of BA), 0.85 (brs, 6H, 2×-CH₃, methyl of BA), 1.67 (s, 3H, 30-CH₃ of BA), 2.48, 2.50, 2.54 (s, each, 3H, 3×-CH₃, methyl of TMP), 2.96–3.01 (m, 1H, -CCHCH₂-), 3.48 (brs, 1H, -CHNH₂), 4.50–4.53 (m, 1H, -OCOCH-), 4.59, 4.71 (brs, each, 1H, =CH₂), 5.17, 5.20 (d, each, 1H, *J* = 15Hz, -OCH₂-); ¹³C-NMR (125 MHz, CDCl₃): δ (ppm) 11.9, 12.0, 14.8, 15.9, 16.0, 16.3, 16.9, 18.3, 19.5, 20.6, 21.0 (-CH₃), 21.5 (-CH₃), 21.8 (-CH₃), 23.9, 24.8, 25.6, 26.2, 28.2, 29.8, 30.7, 32.2, 34.4, 37.1, 37.2, 37.9, 38.2, 38.5, 40.8, 42.5, 47.0, 49.6, 55.6, 56.8 (-CH-NH₂), 59.3, 64.5 (-CH₂), 82.5 (-OCOCH-), 109.8 (-CH=C-), 136.9, 145.5, 148.9, 149.0, 150.6, 151.1 (-CH=C-), 175.7 (-COO-); HRMS (ESI) m/z: 704.52814 [M+H]⁺, calcd. for C₄₄H₆₉N₃O₄ 703.52881.

3β-(L-Pyroglutamyl)-lup-20(29)-ene-28-oic acid-3,5,6-trimethylpyrazin-2-methyl ester (BA-09). Obtained from **TBA** by method A as a colorless powder; Yield: 52.8%; mp: 118.2–119.1 °C, [α]_D = +24 (c 0.50, MeOH); ¹H-NMR (500 MHz, CDCl₃): δ (ppm) 0.78, 0.82, 0.93 (s, each, 3H, 3×-CH₃, methyl of BA), 0.83 (brs, 6H, 2×-CH₃, methyl of BA), 1.67 (s, 3H, 30-CH₃ of BA), 2.48, 2.50, 2.54 (s, each, 3H, 3×-CH₃, methyl of TMP), 2.96–3.01 (m, 1H, -CCHCH₂-), 4.22–4.24 (m, 1H, -NHCH-), 4.52–4.55 (m, 1H, -OCOCH-), 4.59, 4.71 (brs, each, 1H, =CH₂), 5.17, 5.20 (d, each, 1H, *J* = 15Hz, -OCH₂-); ¹³C-NMR (125 MHz, CDCl₃): δ (ppm) 14.8, 16.0, 16.3, 16.7, 18.3, 18.5, 20.5, 21.0 (-CH₃), 21.5 (-CH₃), 21.7 (-CH₃), 23.8, 25.2, 25.6, 28.2, 29.4, 29.7, 29.8, 30.7, 32.1, 34.3, 37.0, 37.2, 38.1, 38.2, 38.4, 40.8, 42.5, 47.0 (-CH-NH-), 49.6, 50.6, 55.5, 55.8, 56.8, 64.4 (-CH₂), 82.7 (-OCOCH-), 109.8 (-CH=C-), 145.6,

148.8, 149.1, 150.6, 151.0 (-CH=C-), 171.7 (-COCH-), 175.7 (-COO-), 177.7
(-CONH-); HRMS (ESI) m/z: 702.48419. [M+H]⁺, calcd. for C₄₃H₆₃N₃O₅ 701. 47677.

3β-(L-Lysyl)-lup-20(29)-ene-28-oic acid-3,5,6-trimethylpyrazin-2-methyl ester
(**BA-10**). Obtained from **TBA** by method A and method C as a colorless powder;
Yield: 56.8%; mp: >220 °C, [α]_D = +30 (c 0.50, MeOH); ¹H-NMR (500 MHz,
CD₃OD): δ (ppm) 0.67, 0.88, 0.89, 0.91, 1.00 (s, each, 3H, 5×-CH₃, methyl of BA),
1.67 (s, 3H, 30-CH₃ of BA), 2.52, 2.53, 2.60 (s, each, 3H, 3×-CH₃, methyl of TMP),
2.93-3.01 (m, 2H, -CH₂NH₂), 3.01-3.04 (m, 1H, -CCHCH₂-), 3.57-3.60 (m, 1H,
-CHNH₂), 4.52-4.55 (m, 1H, -OCOCH-), 4.61, 4.71 (brs, each, 1H, =CH₂), 5.23, 5.27
(d, each, 1H, *J* = 20Hz, -OCH₂-); ¹³C-NMR (125 MHz, CD₃Cl+ CD₃OD): δ (ppm)
14.0, 15.1, 15.5, 15.9, 17.6, 18.5, 19.3 (-CH₃), 20.3 (-CH₃), 20.4 (-CH₃), 21.7, 23.1,
25.0, 26.4, 27.4, 29.1, 30.0, 31.5, 31.6, 33.7, 36.3, 36.6, 37.4, 37.7, 37.9, 38.7, 40.2,
41.9, 46.6, 48.9, 50.0, 52.9, 55.0, 56.3 (-CH-NH₂), 63.5 (-CH₂), 82.5 (-OCOCH-),
111.5 (-CH=C-), 145.2, 148.6, 149.3, 150.0, 150.8 (-CH=C-), 168.7 (-COCH-), 175.4
(-COO-); HRMS (ESI) m/z: 719.54608. [M+H]⁺, calcd. for C₄₄H₇₀N₄O₄ 718.53971.

3β-(L-Tryptophanyl)-lup-20(29)-ene-28-oic acid-3,5,6-trimethylpyrazin-2-methyl
ester (BA-II). Obtained from **TBA** by method A and method C as a colorless powder;
Yield: 61.2%; mp: 119.8–120.6 °C, [α]_D = +30 (c 0.50, MeOH); ¹H-NMR (500 MHz,
CDCl₃): δ (ppm) 0.78 (s, 6H, 2×-CH₃, methyl of BA), 0.83 (s, 6H, 2×-CH₃, methyl of
BA), 0.94 (s, 3H, -CH₃, methyl of BA), 1.67 (s, 3H, 30-CH₃ of BA), 2.49, 2.50, 2.54
(s, each, 3H, 3×-CH₃, methyl of TMP), 2.95-3.02 (m, 2H, -CH₂NH₂), 3.35-3.37 (m,
1H, -CCHCH₂-), 3.70-3.81 (m, 1H, -CHNH₂), 4.45-4.53 (m, 1H, -OCOCH-), 4.68,
4.72 (brs, each, 1H, =CH₂), 5.18, 5.21 (d, each, 1H, *J* = 15Hz, -OCH₂-), 7.05-7.20,
7.29-7.37, 7.60-7.63 (m, 4H, -C₆H₅); ¹³C-NMR (125 MHz, CDCl₃): δ (ppm) 14.8,
16.0, 16.3, 16.7, 18.3, 19.5, 20.6, 21.0 (-CH₃), 21.5 (-CH₃), 21.8 (-CH₃), 23.8, 25.6,
28.1, 29.8, 30.1, 30.7, 32.2, 34.4, 37.1, 37.2, 38.1, 38.2, 38.5, 40.8, 42.5, 47.0, 49.6,
50.6, 54.9, 55.5, 56.8 (-CH-NH₂), 64.5 (-CH₂), 82.5 (-OCOCH-), 109.8 (-CH=C-),
110.3, 111.6, 111.4, 118.8, 119.6, 122.3, 123.8 (-NHCH-), 127.3, 136.5, 145.5, 148.9,
148.9, 150.6, 151.1 (-CH=C-), 175.7 (-CO-); HRMS (ESI) m/z: [M+H]⁺ 777.53125,

calcd. for $C_{49}H_{68}N_4O_4$ 776.52406.

3 β -(L-Sarkosyl)-lup-20(29)-ene-28-oic acid-3,5,6-trimethylpyrazin-2-methyl ester (BA-12). Obtained from **TBA** by method A and method B as a colorless powder; Yield: 76.9%; mp: 172.6–173.4 °C, $[\alpha]_D = +42$ (c 0.50, MeOH); 1H -NMR (500 MHz, $CDCl_3$): δ (ppm) 0.77, 0.84, 0.93 (s, each, 3H, 3 \times -CH₃, methyl of BA), 0.82 (brs, 6H, 2 \times -CH₃, methyl of BA), 1.67 (s, 3H, 30-CH₃ of BA), 2.40, 2.50, 2.53 (s, each, 3H, 3 \times -CH₃, methyl of TMP), 2.96-3.01 (m, 1H, -CCHCH₂-), 3.52 (brs, 2H, -CH₂NH-), 4.48-4.51 (m, 1H, -OCOCH-), 4.56, 4.59 (brs, each, 1H, =CH₂), 5.17, 5.20 (d, each, 1H, $J = 15$ Hz, -OCH₂-); ^{13}C -NMR (125 MHz, $CDCl_3$): δ (ppm) 14.8, 16.0, 16.3, 16.6, 18.3, 19.5, 20.6, 21.0 (-CH₃), 21.5 (-CH₃), 21.8 (-CH₃), 23.9, 25.6, 28.2, 29.8, 30.7, 32.2, 34.4, 34.6, 37.0, 37.2, 38.0, 38.2, 38.5, 40.8, 42.5, 47.0, 49.6, 50.6, 50.7, 55.6, 56.8 (-CH-NH₂), 64.5 (-CH₂), 83.2 (-OCOCH-), 109.8 (-CH=C-), 145.5, 148.9, 149.0, 150.6, 151.1 (-CH=C-), 168.6 (-COCH-), 175.7 (-COO-); HRMS (ESI) m/z : $[M+H]^+$ 662.48975, calcd. for $C_{41}H_{63}N_3O_4$ 661.48186.

3 β -(L-Valyl)-lup-20(29)-ene-28-oic acid-3,5,6-trimethylpyrazin-2-methyl ester (BA-13). Obtained from **TBA** by method A and method C as a colorless powder; Yield: 52.3%; mp: > 220 °C, $[\alpha]_D = +20$ (c 0.50, MeOH); 1H -NMR (500 MHz, $CDCl_3$): δ (ppm) 0.78, 0.82, 0.94 (s, each, 3H, 3 \times -CH₃, methyl of BA), 0.85 (brs, 6H, 2 \times -CH₃, methyl of BA), 1.67 (s, 3H, 30-CH₃ of BA), 2.48, 2.50, 2.54 (s, each, 3H, 3 \times -CH₃, methyl of TMP), 2.96-3.01 (m, 1H, -CCHCH₂-), 3.33-3.34 (m, 1H, -CHNH₂), 4.49-4.52 (m, 1H, -OCOCH-), 4.59, 4.71 (brs, each, 1H, =CH₂), 5.17, 5.20 (d, each, 1H, $J = 15$ Hz, -OCH₂-); ^{13}C -NMR (125 MHz, $CDCl_3$): δ (ppm) 14.8, 16.0, 16.3, 16.8, 18.3, 17.1, 18.3, 19.5, 19.6, 20.6, 21.0 (-CH₃), 21.5 (-CH₃), 21.8 (-CH₃), 23.9, 25.6, 28.2, 29.8, 30.7, 31.6, 32.2, 34.4, 37.1, 37.2, 38.0, 38.2, 38.5, 40.8, 42.5, 47.0, 49.6, 50.6, 55.6, 56.8 (-CH-NH₂), 60.2, 64.5 (-CH₂), 82.2 (-OCOCH-), 109.8 (-CH=C-), 145.5, 148.9, 149.0, 150.6, 151.1 (-CH=C-), 175.7 (-COO-); HRMS (ESI) m/z : $[M+H]^+$ 690.52112, calcd. for $C_{43}H_{67}N_3O_4$ 689.51316.

439 *4.1.2. General Procedure for the Preparation of TBA amino acids derivatives*
 440 **BA-14---BA-15**

441 It was worth noting that, to avoid the formation of by-products, the hydroxyl groups
 442 of Cbz-L-serine Cbz-L-threonine should be protected with TBDMSCl before
 443 esterification with **TBA** in the synthesis of **BA-14** and **BA-15**. To a magnetically
 444 stirred solution of the corresponding N-Cbz-protected amino acid (N-Cbz-L-serine
 445 N-Cbz-L-threonine) (1.0 equiv.) and imidazole (2.0 equiv.) in dry N, N-dimethyl
 446 formamide (10 mL) at 0°C, the TBDMSCl (1.5 equiv.) was added. Then the reaction
 447 mixture was allowed to warm to room temperature and stirred for 24h. After
 448 completion of the reaction (as monitored by TLC), the reaction mixture was poured
 449 into ice-water, and the sediment was filtered and washed with water. Then the residue
 450 was dissolved with DCM, dried over sodium sulfate and evaporated under vacuum,
 451 and the crude product (N-Cbz-TBDMS-L-serine, N-Cbz-TBDMS-L-threonine) was
 452 obtained.

453 The starting material **TBA** (1 equiv.) was dissolved in dry DCM (20 mL), DMAP (0.1
 454 equiv.) and the protected amino acid (1.3 equiv.) were added. After addition of EDCI
 455 (1.5 equiv.), the mixture was stirred at 25 °C for 12 h. Then the solution was washed
 456 with brine. After drying the organic layer over anhydrous Na₂SO₄ and evaporating the
 457 solvent under vacuum, the crude product was purified by flash chromatography (silica
 458 gel, dichloromethane: methanol = 40:1).

459 The Cbz-protected compound was dissolved in 20 mL MeOH, Pd/C (10%; 80 mg)
 460 was added. The mixture was allowed to stir at room temperature for 12 h and filtered
 461 to remove Pd/C. The filtrate was concentrated in vacuum and the residue was further
 462 reacted with 1.5 equivalents of 1M TBAF in THF for 1.5 h at 25 °C. Then the solvent
 463 was evaporated under vacuum. Purification was performed by flash chromatography
 464 (silica gel, dichloromethane: methanol = 40:1).

465 *3β-(L-Threonyl)-lup-20(29)-ene-28-oic acid-3,5,6-trimethylpyrazin-2-methyl ester*
 466 (**BA-14**). Yield: 46.7%; colorless powder; mp: 103.1-103.9 °C, [α]_D = -4 (c 0.50,
 467 MeOH); ¹H-NMR (500 MHz, CDCl₃): δ (ppm) 0.78, 0.85, 0.86 (s, each, 3H, 3×-CH₃,

468 methyl of BA), 0.82 (brs, 6H, 2×-CH₃, methyl of BA), 1.67 (s, 3H, 30-CH₃ of BA),
 469 2.48, 2.50, 2.54 (s, each, 3H, 3×-CH₃, methyl of TMP), 2.97-3.00 (m, 1H, -CCHCH₂-),
 470 3.39-3.58 (m, 1H, -CHNH₂), 3.85-3.98 (m, 1H, -CHOH), 4.54-4.55 (m, 1H,
 471 -OCOCH-), 4.58, 4.71 (brs, each, 1H, =CH₂), 5.16, 5.19 (d, each, 1H, *J* = 15Hz,
 472 -OCH₂-); ¹³C-NMR (125 MHz, CDCl₃): δ (ppm) 14.8, 16.0, 16.3, 16.8, 18.3, 19.5
 473 (CH₃CH-), 20.6, 21.0 (-CH₃), 21.5 (-CH₃), 21.8 (-CH₃), 23.9, 25.5, 27.7, 28.2, 29.0,
 474 29.7, 30.6, 32.1, 34.3, 37.0, 37.2, 38.0, 38.2, 38.5, 40.8, 42.5, 47.0, 49.6, 50.5, 55.6
 475 (-CH-NH₂), 56.8, 64.5 (-CH₂), 67.2 (-CHOH), 82.6 (-OCOCH-), 95.8, 109.8
 476 (-CH=C-), 145.5, 148.9, 149.0, 150.6, 151.1 (-CH=C-), 175.75 (-CO-); HRMS (ESI)
 477 *m/z*: [M+H]⁺ 692.49957, calcd. for C₄₂H₆₅N₃O₅ 691.49242.

478 *3β-(L-Seryl)-lup-20(29)-ene-28-oic acid-3,5,6-trimethylpyrazin-2-methyl ester*
 479 (**BA-15**). Yield: 47.5%; colorless powder; mp: 133.2-134.1 °C, [α]_D = +16 (c 0.50,
 480 MeOH); ¹H-NMR (500 MHz, CDCl₃): δ (ppm) 0.77, 0.82, 0.93 (s, each, 3H, 3×-CH₃,
 481 methyl of BA), 0.83 (brs, 6H, 2×-CH₃, methyl of BA), 1.66 (s, 3H, 30-CH₃ of BA),
 482 2.48, 2.50, 2.53 (s, each, 3H, 3×-CH₃, methyl of TMP), 2.97-3.00 (m, 1H, -CCHCH₂-),
 483 3.32-3.35 (s, 1H, -CHNH₂), 3.63 (brs, 1H, -OH), 3.72-3.75 (m, 1H, -CH₂OH),
 484 3.86-3.94 (m, 1H, -CH₂OH), 4.52-4.56 (m, 1H, -OCOCH-), 4.58, 4.71 (brs, each, 1H,
 485 =CH₂), 5.16, 5.19 (d, each, 1H, *J* = 15Hz, -OCH₂-); ¹³C-NMR (125 MHz, CDCl₃): δ
 486 (ppm) 14.8, 16.0, 16.3, 16.7, 18.3, 19.5, 20.6, 21.0 (-CH₃), 21.5 (-CH₃), 21.8 (-CH₃),
 487 23.9, 24.3, 25.5, 28.1, 29.7, 30.6, 32.1, 34.3, 37.0, 37.2, 38.1, 38.2, 38.4, 40.8, 42.5,
 488 47.0, 49.6, 50.5, 55.5 (-CH-NH₂), 56.8, 62.5 (-CH₂OH), 64.5 (-CH₂), 82.4
 489 (-OCOCH-), 82.7, 109.8 (-CH=C-), 145.5, 148.9, 149.0, 150.6, 151.1 (-CH=C-),
 490 175.7 (-COO-); HRMS (ESI) *m/z*: [M+H]⁺ 678.48480, calcd. for C₄₁H₆₃N₃O₅
 491 677.47677.

492 4.1.3. General Procedure for the Preparation of TBA dipeptide derivatives 493 **BA-16---BA-27**

494 The corresponding TBA amino acid derivatives (**BA-02**, **BA-04**, **BA-06**, **BA-12**) (1.0
 495 equiv.), DMAP (0.1 equiv.) and N-Boc-protected amino acids (Boc-L-glycine,
 496 Boc-L-alanine, Boc-L-sarcosine, Boc-L-proline) were dissolved in 25 mL dry DCM,

EDCI (0.1 equiv.) was added. The mixture was stirred at room temperature overnight. Then the solution was washed with brine, dried over sodium sulfate, filtered and the solvent was evaporated. Purification was performed by flash chromatography (silica gel, dichloromethane: methanol = 40:1). Then the Boc-protected compounds were further reacted with TFA (1 mL per 10 mL DCM) in dry DCM in ice bath for 2 h. After completion of the reaction (as monitored by TLC), the solution was evaporated and washed with a saturated sodium carbonate solution (20 mL). The aqueous layer was extracted with DCM (3 × 25 mL), the combined organic extracts were washed with brine (20 mL), dried over sodium sulfate, filtrated and evaporated. Purification was performed by flash chromatography (silica gel, dichloromethane: methanol = 30:1).

3β-[(L-Glycyl)-L-Glycyl]-lup-20(29)-ene-28-oic acid-3,5,6-trimethylpyrazin-2-methyl ester (BA-16). Yield: 52.8%; colorless powder; mp: 130.8-131.7 °C, $[\alpha]_D = +15$ (c 0.50, MeOH); $^1\text{H-NMR}$ (500 MHz, CD_3OD): δ (ppm) 0.67, 0.98 (s, each, 3H, 2×-CH₃, methyl of BA), 0.88 (brs, 9H, 3×-CH₃, methyl of BA), 1.67 (s, 3H, 30-CH₃ of BA), 2.52, 2.53, 2.60 (s, each, 3H, 3×-CH₃, methyl of TMP), 2.98-3.04 (m, 1H, -CCHCH₂-), 3.35 (s, 2H, -CH₂NH₂), 3.98 (s, 2H, -CH₂NH-), 4.50-4.53 (m, 1H, -OCOCH-), 4.61, 4.71 (brs, each, 1H, =CH₂), 5.23, 5.26 (d, each, 1H, $J = 15\text{Hz}$, -OCH₂-), 5.51 (s, 1H, -NH-). $^{13}\text{C-NMR}$ (125 MHz, CD_3OD): δ (ppm) 15.1, 16.4, 16.7, 16.9, 19.2, 19.5, 20.4, 21.2 (-CH₃), 21.4 (-CH₃), 22.0 (-CH₃), 24.6, 26.7, 28.4, 30.7, 31.6, 33.1, 35.4, 37.8, 38.2, 39.0, 39.6, 41.9 (-CH₂-NH-), 42.1, 43.5 (-CH₂-NH₂), 45.6, 50.6, 51.7, 54.8, 56.8, 57.9, 65.0 (-CH₂), 83.4 (-OCOCH-), 110.4 (-CH=C-), 147.1, 150.3, 150.7, 151.7, 152.5 (-CH=C-), 160.0, 171.3 (-CONH-), 175.7 (-COCH₂-), 177.0 (-COO-); HRMS (ESI) m/z : $[\text{M}+\text{H}]^+$ 705.49500, calcd. for $\text{C}_{42}\text{H}_{64}\text{N}_4\text{O}_5$ 704.48767.

3β-[(L-Sarkosyl)-L-Sarkosyl]-lup-20(29)-ene-28-oic acid-3,5,6-trimethylpyrazin-2-methyl ester (BA-17). Yield: 62.3%; colorless powder; mp: 118.4-119.2 °C, $[\alpha]_D = +12$ (c 0.50, MeOH); $^1\text{H-NMR}$ (500 MHz, CDCl_3): δ (ppm) 0.76, 0.81, 0.93 (s, each, 3H, 3×-CH₃, methyl of BA), 1.66 (s, 3H, 30-CH₃ of BA), 2.48, 2.50, 2.53 (s, each, 3H, 3×-CH₃, methyl of TMP), 3.04-3.17 (m, 2H, -CH₂NH-), 2.98 (s, 3H, CH₃-N-), 2.98-3.04 (m, 1H, -CCHCH₂-), 3.96 (s, 3H,

CH₃-NH-), 3.96-4.12 (m, 2H, -CH₂N-), 4.50-4.51 (m, 1H, -OCOCH-), 4.58, 4.70 (brs, each, 1H, =CH₂), 5.16, 5.19 (d, each, 1H, *J* = 15Hz, -OCH₂-); ¹³C-NMR (125 MHz, CDCl₃): δ (ppm) 14.8, 16.0, 16.3, 16.7, 18.4, 19.5, 21.0 (-CH₃), 21.5 (-CH₃), 21.8 (-CH₃), 23.8, 25.6, 28.1, 29.7, 30.7, 32.2, 33.4, 34.4, 35.8 (CH₃N-), 37.0, 37.3, 38.0, 38.2, 38.8, 39.0, 40.8, 42.5, 47.0, 49.6, 50.6, 51.8, 55.4 (-CH-NH₂), 56.8, 64.5 (-CH₂), 79.1 (CH₃NH-), 82.9 (-OCOCH-), 109.7 (-CH=C-), 145.5, 148.9, 149.0, 150.7, 151.1 (-CH=C-), 163.3, 168.4 (-CH₂COO-), 175.7 (-CO-); HRMS (ESI) *m/z*: [M+H]⁺ 733.52527, calcd. for C₄₄H₆₅N₃O₅ 732.51897.

3β-[(L-Prolyl)-L-Sarkosyl]-lup-20(29)-ene-28-oic acid-3,5,6-trimethylpyrazin-2-methyl ester (BA-18). Yield: 60.7%; colorless powder; mp: 158.5-159.3 °C, [α]_D = +52 (c 0.50, MeOH); ¹H-NMR (500 MHz, CDCl₃): δ (ppm) 0.78, 0.81, 0.93 (s, each, 3H, 3×-CH₃, methyl of BA), 0.82 (s, 6H, 2×-CH₃, methyl of BA), 1.67 (s, 3H, 30-CH₃ of BA), 2.50, 2.53, 2.56 (s, each, 3H, 3×-CH₃, methyl of TMP), 2.95-2.99 (m, 1H, -CCHCH₂-), 3.11 (s, 3H, CH₃N-), 3.42, 3.46 (brs, each, 1H, -CH₂-NH-), 3.68-3.71 (m, 1H, -CHNH-), 4.51-4.53 (m, 1H, -OCOCH-), 4.59, 4.71 (brs, each, 1H, =CH₂), 5.18, 5.21 (d, each, 1H, *J* = 15Hz, -OCH₂-); ¹³C-NMR (125 MHz, CDCl₃): δ (ppm) 14.8, 16.0, 16.3, 16.7, 18.3, 19.5, 20.4, 21.0 (-CH₃), 21.5 (-CH₃), 21.8 (-CH₃), 23.9, 25.6, 28.2, 29.4, 29.8, 30.7, 32.1, 34.3, 36.4, 37.0, 37.2, 38.0, 38.2, 38.5, 40.8, 42.5, 47.0, 49.6, 50.4, 50.6, 55.5, 56.8, 58.3, 62.4, 64.4 (-CH₂), 83.1 (-OCOCH-), 109.8 (-CH=C-), 145.8, 148.6, 149.3, 150.6, 151.1 (-CH=C-), 163.3, 168.0 (-CH₂COO-), 169.3 (-CON-), 175.6 (-COO-); HRMS (ESI) *m/z*: [M+H]⁺ 759.54059, calcd. for C₄₆H₇₀N₄O₅ 758.53462.

3β-[(L-Alanyl)-L-Glycyl]-lup-20(29)-ene-28-oic acid-3,5,6-trimethylpyrazin-2-methyl ester (BA-19). Yield: 58.9%; colorless powder; mp: 117.8-118.7°C, [α]_D = +17 (c 0.50, MeOH); ¹H-NMR (500 MHz, CDCl₃): δ (ppm) 0.77, 0.83, 0.93 (s, each, 3H, 3×-CH₃, methyl of BA), 0.82 (s, 6H, 2×-CH₃, methyl of BA), 1.67 (s, 3H, 30-CH₃ of BA), 2.48, 2.50, 2.53 (s, each, 3H, 3×-CH₃, methyl of TMP), 2.87-2.95 (s, each, 2H, -NH₂-), 2.96-3.01 (m, 1H, -CCHCH₂-), 3.61-3.63 (m, 1H, -CH-), 4.01 (d, 2H, -NHCH₂-), 4.50-4.53 (m, 1H, -CHCH₃), 4.58, 4.70 (brs, each, 1H, =CH₂), 5.17, 5.20 (d, each, 1H,

555 $J = 15\text{Hz}$, $-\text{OCH}_2-$), 7.80 (s, 1H, $-\text{NH}-\text{CH}_2-$); ^{13}C -NMR (125 MHz, CDCl_3): δ (ppm)
 556 14.8, 16.0, 16.3, 16.6, 18.3, 19.5, 21.0, 20.6 ($-\text{CH}_3$), 21.4, 21.5 ($-\text{CH}_3$), 21.8 ($-\text{CH}_3$),
 557 23.8, 25.6, 28.1, 29.7, 30.7, 32.2, 34.4, 37.0, 37.2, 38.0, 38.2, 38.5, 39.0, 40.8, 41.4
 558 ($-\text{NH}-\text{CH}_2-$), 42.5, 47.0, 49.6, 50.6 ($-\text{CHNH}_2$), 50.7, 55.5, 56.8, 64.5 ($-\text{CH}_2$), 82.6,
 559 109.8 ($-\text{CH}=\text{C}-$), 145.5, 148.9, 149.0, 150.6, 151.1 ($-\text{CH}=\text{C}-$), 169.9 ($-\text{CH}_2-\text{COO}-$),
 560 175.7 ($-\text{COO}-$); HRMS (ESI) m/z : $[\text{M}+\text{H}]^+$ 719.51080, calcd. for $\text{C}_{43}\text{H}_{66}\text{N}_4\text{O}_5$
 561 718.50332.

562 3β -[(*L*-Prolyl)-*L*-Glycyl]-lup-20(29)-ene-28-oic acid-3,5,6-trimethylpyrazin-2-methyl
 563 ester (**BA-20**). Yield: 59.3%; colorless powder; mp: 122.6-123.5 °C, $[\alpha]_{\text{D}} = +4$ (c 0.50,
 564 MeOH); ^1H -NMR (500 MHz, CDCl_3): δ (ppm) 0.77, 0.83, 0.93 (s, each, 3H, $3\times\text{-CH}_3$,
 565 methyl of BA), 0.82 (s, 6H, $2\times\text{-CH}_3$, methyl of BA), 1.67 (s, 3H, 30-CH_3 of BA), 2.48,
 566 2.50, 2.53 (s, each, 3H, $3\times\text{-CH}_3$, methyl of TMP), 2.99-3.03 (m, 2H, $-\text{CH}_2\text{NH}-$),
 567 3.07-3.12 (m, 1H, $-\text{CCHCH}_2-$), 3.94-3.97 (m, 1H, $-\text{NHCH}-$), 4.00-4.02 (m, 2H,
 568 $-\text{CH}_2\text{CH}_2-$), 4.49-4.52 (m, 1H, $-\text{OCOCH}-$), 4.58, 4.71 (brs, each, 1H, $=\text{CH}_2$), 5.17,
 569 5.20 (d, each, 1H, $J = 15\text{Hz}$, $-\text{OCH}_2-$), 8.19 (s, 1H, $-\text{NH}-$); ^{13}C -NMR (125 MHz,
 570 CDCl_3): δ (ppm) 14.8, 16.0, 16.3, 16.6, 18.3, 19.5, 20.6, 21.0 ($-\text{CH}_3$), 21.5 ($-\text{CH}_3$),
 571 21.8 ($-\text{CH}_3$), 23.8, 25.6, 26.1, 28.2, 29.8, 30.7, 30.8, 32.2, 34.4, 37.1, 37.2, 38.0, 38.2,
 572 38.5, 40.8 ($-\text{NHCH}-$), 41.4, 42.5, 47.0, 47.3, 49.6, 50.6, 55.5, 56.8, 60.5, 62.4
 573 ($-\text{CHNH}-$), 64.5 ($-\text{CH}_2$), 82.6 ($-\text{OCOCH}-$), 109.8 ($-\text{CH}=\text{C}-$), 145.5, 148.9, 150.6,
 574 151.1 ($-\text{CH}=\text{C}-$), 169.9 ($-\text{CONH}-$), 175.7 ($-\text{COOCH}-$), 175.7 ($-\text{COO}-$); HRMS (ESI)
 575 m/z : $[\text{M}+\text{H}]^+$ 745.52527, calcd. for $\text{C}_{45}\text{H}_{68}\text{N}_4\text{O}_5$ 744.51897.

576 3β -[(*L*-Sarkosyl)-*L*-Glycyl]-lup-20(29)-ene-28-oic
 577 acid-3,5,6-trimethylpyrazin-2-methyl ester (**BA-21**). Yield: 57.6%; colorless powder;
 578 mp: 117.8-118.6 °C, $[\alpha]_{\text{D}} = +16$ (c 0.50, MeOH); ^1H -NMR (500 MHz, CDCl_3): δ
 579 (ppm) 0.77 (s, each, 3H, $-\text{CH}_3$, methyl of BA), 0.82 (brs, 9H, $3\times\text{-CH}_3$, methyl of BA),
 580 0.93 (s, 6H, $2\times\text{-CH}_3$, methyl of BA), 1.67 (s, 3H, 30-CH_3 of BA), 2.48, 2.50, 2.53 (s,
 581 each, 3H, $3\times\text{-CH}_3$, methyl of TMP), 2.97-3.01 (m, 1H, $-\text{CCHCH}_2-$), 3.32 (s, 2H,
 582 $-\text{NHCH}_2-$), 3.78-4.03 (m, 2H, $-\text{CH}_2\text{CO}-$), 4.50-4.53 (m, 1H, $-\text{OCOCH}-$), 4.58, 4.71
 583 (brs, each, 1H, $=\text{CH}_2$), 5.16, 5.19 (d, each, 1H, $J = 15\text{Hz}$, $-\text{OCH}_2-$); ^{13}C -NMR (125

584 MHz, CDCl₃): δ (ppm) 14.8, 16.0, 16.3, 16.6, 18.3, 19.4, 20.6, 21.0 (-CH₃), 21.5
 585 (-CH₃), 21.8 (-CH₃), 21.9, 22.0, 23.7, 25.6, 28.0, 29.7, 30.7, 32.2, 34.4, 34.6, 37.0,
 586 37.2, 38.0, 38.2, 38.5, 40.8, 42.5, 47.0, 49.6, 50.6, 55.5 (-NHCH₂-), 56.8, 64.5 (-CH₂),
 587 82.6 (-OCOCH-), 109.8 (-CH=C-), 145.5, 148.9, 149.0, 150.1, 151.1 (-CH=C-), 168.6
 588 (-CONH-), 170.8 (-COOCH-), 175.7 (-COO-); HRMS (ESI) m/z: [M+H]⁺ 719.51044,
 589 calcd. for C₄₃H₆₆N₄O₅ 718.50332.

590 *3 β -[(L-Alanyl)-L-Alanyl]-lup-20(29)-ene-28-oic acid-3,5,6-trimethylpyrazin-2-methyl*
 591 *ester (BA-22)*. Yield: 53.1%; colorless powder; mp: 118.3-119.2 °C, [α]_D = -2 (c 0.50,
 592 MeOH); ¹H-NMR (500 MHz, CDCl₃): δ (ppm) 0.78, 0.94 (s, each, 3H, 2 \times -CH₃,
 593 methyl of BA), 0.82-0.83 (m, 9H, 3 \times -CH₃, methyl of BA), 1.67 (s, 3H, 30-CH₃ of
 594 BA), 2.48, 2.50, 2.54 (s, each, 3H, 3 \times -CH₃, methyl of TMP), 2.96-3.01 (m, 1H,
 595 -CCHCH₂-), 3.56-3.60 (m, 1H, NH₂CH-), 4.49-4.52 (m, 1H, -OCOCH-), 4.52-4.57
 596 (m, 1H, -NHCH-), 4.58, 4.71 (brs, each, 1H, =CH₂), 5.17, 5.20 (d, each, 1H, *J* = 15Hz,
 597 -OCH₂-), 7.75-7.76 (d, 1H, -NH-); ¹³C-NMR (125 MHz, CDCl₃): δ (ppm) 14.8, 16.0,
 598 16.3, 16.7, 18.3, 18.7, 19.5, 20.6, 21.0 (-CH₃), 21.5 (-CH₃), 21.8 (-CH₃), 23.8, 25.6,
 599 28.1, 29.8, 30.7, 32.2, 34.4, 37.1, 37.2, 38.1, 38.2, 38.4, 40.8, 41.6, 42.5, 47.0, 48.4
 600 49.6 (NH₂CH-), 50.6, 55.5, 56.8 (-NHCH-), 64.5 (-CH₂), 82.4 (-OCOCH-), 109.8
 601 (-CH=C-), 145.5, 148.9, 149.0, 150.1, 151.1 (-CH=C-), 172.8 (-COOCH-), 175.7
 602 (-COO-); HRMS (ESI) m/z: [M+H]⁺ 733.52606, calcd. for C₄₄H₆₈N₄O₅ 732.51897.

603 *3 β -[(L-Glycyl)-L-Alanyl]-lup-20(29)-ene-28-oic acid-3,5,6-trimethylpyrazin-2-methyl*
 604 *ester (BA-23)*. Yield: 55.3%; colorless powder; mp: 172.4-173.3 °C, [α]_D = -2 (c 0.50,
 605 MeOH); ¹H-NMR (500 MHz, CDCl₃): δ (ppm) 0.78, 0.83, 0.94 (s, each, 3H, 3 \times -CH₃,
 606 methyl of BA), 0.82 (s, 6H, 2 \times -CH₃, methyl of BA), 1.67 (s, 3H, 30-CH₃ of BA), 2.48,
 607 2.50, 2.54 (s, each, 3H, 3 \times -CH₃, methyl of TMP), 2.97-3.01 (m, 1H, -CCHCH₂-), 3.56
 608 (brs, 2H, -CH₂NH₂), 4.49-4.52 (m, 1H, -OCOCH-), 4.58 (m, 1H, -NHCH-), 4.58, 4.71
 609 (brs, each, 1H, =CH₂), 5.17, 5.20 (d, each, 1H, *J* = 15Hz, -OCH₂-), 7.87 (s, 1H, -NH-);
 610 ¹³C-NMR (125 MHz, CDCl₃): δ (ppm) 14.8, 16.0, 16.3, 16.7, 18.3, 18.8, 19.5, 20.6,
 611 21.0 (-CH₃), 21.5 (-CH₃), 21.8 (-CH₃), 23.8, 25.6, 28.1, 29.8, 30.7, 32.2, 34.4, 37.1,
 612 37.2, 38.1, 38.2, 38.4, 40.8, 42.5 (NH₂CH₂-), 47.0, 48.2, 49.6, 50.6, 50.7, 55.5

613 (-NHCH-), 56.8, 64.5 (-CH₂), 82.3 (-OCOCH-), 109.8 (-CH=C-), 145.5, 148.9, 149.0,
 614 150.6, 151.1 (-CH=C-), 172.9 (-COCH-), 175.7 (-COO-); HRMS (ESI) m/z: [M+H]⁺
 615 719.51044, calcd. for C₄₃H₆₆N₄O₅ 718.50332.

616 *3β-[(L-Prolyl)-L-Alanyl]-lup-20(29)-ene-28-oic acid-3,5,6-trimethylpyrazin-2-methyl*
 617 *ester (BA-24)*. Yield: 56.4%; colorless powder; mp: 113.7-114.5 °C, [α]_D = -6 (c 0.50,
 618 MeOH); ¹H-NMR (500 MHz, CDCl₃): δ (ppm) 0.77, 0.79, 0.93 (s, each, 3H, 3×-CH₃,
 619 methyl of BA), 0.81-0.86 (m, 6H, 2×-CH₃, methyl of BA), 1.67 (s, 3H, 30-CH₃ of
 620 BA), 2.48, 2.49, 2.53 (s, each, 3H, 3×-CH₃, methyl of TMP), 2.65-2.70 (m, 1H,
 621 -NHCH-), 2.91-3.03 (m, 2H, -CH₂NH-), 3.04-3.08 (m, 1H, -CCHCH₂-), 3.82-3.83 (m,
 622 1H, -CHNH-), 4.47-4.56 (m, 1H, -OCOCH-), 4.70, 4.73 (brs, each, 1H, =CH₂), 5.16,
 623 5.19 (d, each, 1H, *J* = 15Hz, -OCH₂-), 8.07-8.09 (d, 1H, -NH-); ¹³C-NMR (125 MHz,
 624 CDCl₃): δ (ppm) 14.8, 16.0, 16.3, 16.7, 18.3, 19.5, 20.6, 21.0 (-CH₃), 21.5 (-CH₃),
 625 21.8 (-CH₃), 23.8, 25.6, 28.1, 29.7, 30.7, 31.0, 32.2, 34.3, 37.0, 37.2, 38.0, 38.2, 38.5,
 626 40.8, 42.5, 47.0, 47.3, 49.6, 50.0, 50.6 (-NHCH-), 55.5, 56.8, 60.5, 62.8, 64.5 (-CH₂),
 627 78.9, 82.2 (-OCOCH-), 109.8 (-CH=C-), 145.5, 148.9, 149.0, 150.6, 151.1 (-CH=C-),
 628 170.8 (-CONH-), 174.7 (-COOCH-), 175.7 (-COO-); HRMS (ESI) m/z: [M+H]⁺
 629 759.54053, calcd. for C₄₆H₇₀N₄O₅ 758.53462.

630 *3β-[(L-Sarkosyl)-L-Alanyl]-lup-20(29)-ene-28-oic*
 631 *acid-3,5,6-trimethylpyrazin-2-methyl ester (BA-25)*. Yield: 58.7%; colorless powder;
 632 mp: 136.5-137.3 °C, [α]_D = -2 (c 0.50, MeOH); ¹H-NMR (500 MHz, CDCl₃): δ (ppm)
 633 0.77, 0.83, 0.93 (s, each, 3H, 3×-CH₃, methyl of BA), 0.82 (s, 6H, 2×-CH₃, methyl of
 634 BA), 1.67 (s, 3H, 30-CH₃ of BA), 2.48, 2.50, 2.53 (s, each, 3H, 3×-CH₃, methyl of
 635 TMP), 2.63-2.73 (m, 1H, -NHCH-) 2.94-3.01 (m, 1H, -CCHCH₂-), 3.35-3.44 (m, 2H,
 636 -NHCH₂-), 4.48-4.51 (m, 1H, -OCOCH-), 4.58, 4.71 (brs, each, 1H, =CH₂), 5.17, 5.20
 637 (d, each, 1H, *J* = 15Hz, -OCH₂-), 7.80-7.82 (d, 1H, -NH-); ¹³C-NMR (125 MHz,
 638 CDCl₃): δ (ppm) 14.8, 16.0, 16.3, 16.7, 18.3, 18.7, 19.5, 20.6, 21.0 (-CH₃), 21.5
 639 (-CH₃), 21.8 (-CH₃), 23.8, 25.6, 28.1, 29.8, 30.7, 32.2, 34.4, 36.2, 37.1, 37.2, 38.1,
 640 38.2, 38.4, 40.8, 42.5, 47.0, 48.2, 49.6, 50.6, 53.7, 55.5, 56.8, 64.5 (-CH₂), 82.4
 641 (-OCOCH-), 109.8 (-CH=C-), 145.5, 148.9, 149.0, 150.6, 151.1 (-CH=C-), 172.7

642 (-CONH-), 175.7 (-COO-); HRMS (ESI) m/z: [M+H]⁺ 733.52521, calcd. for
 643 C₄₄H₆₈N₄O₅ 732.51897.

644 *3β-[(L-Glycyl)-L-Sarkosyl]-lup-20(29)-ene-28-oic*

645 *acid-3,5,6-trimethylpyrazin-2-methyl ester (BA-26)*. Yield: 78.5%; colorless powder;
 646 mp: 117.2-118.1 °C, [α]_D = +14 (c 0.50, MeOH); ¹H-NMR (500 MHz, CDCl₃): δ
 647 (ppm) 0.77, 0.79, 0.93 (s, each, 3H, 3×-CH₃, methyl of BA), 0.81 (s, 6H, 2×-CH₃,
 648 methyl of BA), 1.67 (s, 3H, 30-CH₃ of BA), 2.48, 2.50, 2.53 (s, each, 3H, 3×-CH₃,
 649 methyl of TMP), 2.97-3.01 (m, 1H, -CCHCH₂-), 3.00-3.06 (m, 2H, -CH₂NH₂),
 650 3.95-4.13 (m, 3H, CH₃NH-), 4.48-4.56 (m, 2H, -CH₂-), 4.58, 4.70 (brs, each, 1H,
 651 =CH₂), 5.16, 5.20 (d, each, 1H, *J* = 15Hz, -OCH₂-); ¹³C-NMR (125 MHz, CDCl₃): δ
 652 (ppm) 14.8, 15.5, 16.0, 16.3, 16.7, 18.3, 19.5, 20.6, 21.0 (-CH₃), 21.5 (-CH₃), 21.8
 653 (-CH₃), 25.6, 28.1, 28.2, 29.8, 30.7, 31.1, 32.2, 34.4, 37.1, 37.2, 37.3, 38.0, 38.2, 38.5,
 654 40.8, 42.5 (-CH₂NH₂), 47.0, 49.6, 50.6, 55.5, 56.8 (-NCH₂-), 64.5 (-CH₂), 79.1, 109.8
 655 (-CH=C-), 145.5, 148.9, 149.0, 150.6, 151.1 (-CH=C-), 175.7 (-COOCH₂-); HRMS
 656 (ESI) m/z: [M+H]⁺ 719.51044, calcd. for C₄₃H₆₆N₄O₅ 718.50332.

657 *3β-[(L-Alanyl)-L-Sarkosyl]-lup-20(29)-ene-28-oic*

658 *acid-3,5,6-trimethylpyrazin-2-methyl ester (BA-27)*. Yield: 79.8%; colorless powder;
 659 mp: 136.2-137.1 °C, [α]_D = +34 (c 0.50, MeOH); ¹H-NMR (500 MHz, CDCl₃): δ
 660 (ppm) 0.78, 0.93 (s, each, 3H, 2×-CH₃, methyl of BA), 0.81 (s, 9H, 3×-CH₃, methyl of
 661 BA), 1.67 (s, 3H, 30-CH₃ of BA), 2.48, 2.49, 2.53 (s, each, 3H, 3×-CH₃, methyl of
 662 TMP), 2.87, 2.95 (s, each, 2H, -CH₂-), 4.01 (brs, 2H, -CNH₂), 4.06 (brs, 3H, -NCH₃),
 663 4.58, 4.70 (brs, each, 1H, =CH₂), 5.16, 5.20 (d, each, 1H, *J* = 15Hz, -OCH₂-);
 664 ¹³C-NMR (125 MHz, CDCl₃): δ (ppm) 14.8, 16.0, 16.3, 16.7, 18.3, 19.5, 19.6, 20.6,
 665 21.0 (-CH₃), 21.5 (-CH₃), 21.8 (-CH₃), 23.8, 25.6, 28.2, 29.8, 30.7, 31.6, 32.2, 34.4,
 666 36.6 (-NCH₃), 37.0, 37.2, 38.0, 38.2, 38.5, 40.8, 41.6, 42.5, 47.0, 49.6, 50.2, 50.6,
 667 55.5, 56.8 (-NCH₂-), 64.5 (-CH₂), 82.7, 109.81 (-CH=C-), 145.5, 148.9, 149.0, 150.6,
 668 151.1 (-CH=C-), 162.7 (-CH₂-COO-), 175.6 (-COOCH₂-); HRMS (ESI) m/z: [M+H]⁺
 669 733.52545, calcd. for C₄₄H₆₈N₄O₅ 732.51897.

4.2. Bio-Evaluation Methods

4.2.1. Cell Culture

The human hepatocellular carcinoma cell line (HepG2), human colon carcinoma cell line (HT-29), human cervical cancer cell line (Hela), human lung cancer cell line (A549), human gastric cancer cell line (BGC-823) and Madin-Darby canine kidney cell line (MDCK) were obtained from the Chinese Academy of Medical Sciences & Peking Union Medical College. The cultures of the cells were maintained as monolayer in RPMI 1640 supplemented with 10% (v/v) heat inactivated fetal bovine serum and 1% (v/v) enicillin/streptomycin (Thermo Technologies, New York, NY, USA) and incubated at 37 °C in a humidified atmosphere with 5% CO₂. The **TBA** derivatives under study were dissolved in DMSO (Sigma, St. Louis, MO, USA) and added at required concentrations to the cell culture.

4.2.2. Cytotoxicity Assay

The cytotoxicity of the compounds was evaluated *in vitro* via the MTT method against HepG2, HT-29, Hela, BGC-823, A-549 cell lines with cisplatin as the positive control. Tumor cells growing in the logarithmic phase were seeded in 96-well plates at a density 3×10^3 cells/well and incubated overnight. The following day, cells were then treated with serial dilutions of the tested compounds for 72h. At the end of this incubation, 20μL of 5 mg/mL methylthiazol tetrazolium (MTT) was added to each well and incubation proceeded at 37°C for another 4 h. After the supernatant medium was thrown away, 150 μL dimethylsulphoxide (DMSO) were added to each well and absorbance was measured at 490 nm using a plate reader (BIORAD 550 spectrophotometer, Bio-rad Life Science Development Ltd., Beijing, China). Experiments were performed in triplicates and the values were the average of three ($n = 3$) independent experiments. The concentration of the compound which gives 50% growth inhibition corresponds to the IC₅₀. Tumor cell growth inhibitory rate was calculated in the following Equation (1):

$$\% \text{ inhibition} = (1 - \text{Sample group OD} / \text{Control group OD}) \times 100\% \quad (1)$$

4.2.3. Morphological detection of apoptosis using Giemsa staining

To observe the changes in cell morphology after treatment with **BA-25**, Giemsa staining was performed as previously described [19]. Briefly, exponentially growing

HepG2 cells (4×10^3 cells/well) were cultured in 6-well plates overnight and then treated with various concentrations of **BA-25** (1.5, 3, 6 μ M) for an additional 72 h. Following twice washes with PBS and fixing with cold methanol, cells were stained with 6% Giemsa (Giemsa, Molecular Probes/Invitrogen Life Technologies, Carlsbad, CA, USA) solution for 5 min, washed with water and dried. The cell morphological changes were observed under a fluorescent microscope [38].

4.2.4. Morphological detection of apoptosis using DAPI staining

Morphological observation of nuclear changes was performed by DAPI staining in this assay. HepG2 cells were seeded in the six well plates at a density of 4×10^3 cells/well and were allowed to grow for 12 h. Then the cells were treated with different concentration ranges of **BA-25** (1.5, 3, 6 μ M) for 72 hours. After the treatment period, cells were washed with PBS and fixed with 4% paraformaldehyde. Then the liquid was removed and the cells were stained with 1 mg/mL DAPI (DAPI, Molecular Probes/Invitrogen Life Technologies, Carlsbad, CA, USA) for 1 min in dark. After staining, cells were visualised under a fluorescence microscope [39].

4.2.5. Detection of apoptosis using Annexin V-FITC/PI staining

To determine early apoptosis and secondary necrosis, HepG2 cells were stained with annexin-V FITC apoptosis detection kit (Beijing BioDee Biotech. Co., Ltd., Beijing, China) as per manufacturer instruction. After exposure to **BA-25** (2, 3, 4 μ M) for 72 h, HepG2 cells were collected, washed twice with cold PBS and centrifuged at 1000 rpm for 5 min. The resulting pellet was mixed with 200 μ L binding buffer of the Annexin V-FITC kit, then 10 μ L FITC labeled annexin V was added and mixed gently. After incubation at 4°C for 15min in the dark, the cells were washed twice and resuspended in 300 μ L binding buffer containing 10 μ L PI. Then the cells were immediately analyzed with a flow cytometry [40].

4.2.6. Measurement of mitochondrial membrane potential

Evaluation of mitochondrial membrane potential in HepG2 cells was performed by flow cytometry using the rhodamine 123 (Rh123) staining. HepG2 cells (1×10^5 cells/well) in logarithmic growth phase were incubated in 6-well culture plate for 24 h. Then the cells were exposed to 2, 3 and 4 μ M **BA-25** for 72h and harvested by

trypsinization. After twice washes with cold PBS, the cells were incubated at 37°C with 10 µg/mL Rh123 (Rh123, Beijing BioDee Biotech. Co., Ltd., Beijing, China) for 30 min. Following twice washes with PBS, fluorescent intensities were determined by flow cytometry with excitation and emission wavelength set at 488 nm and 530 nm, respectively [33, 36].

4.2.7. Assessment of intracellular Free Ca^{2+}

For the measurement of intracellular free Ca^{2+} , HepG2 cells were seeded in 6-well plate at 1×10^5 cells/well and were allowed to grow for 24h. After **BA-25** (2, 3, 4 µM) treatment for 72h, the cells were harvested and washed twice with cold PBS, then resuspended in HBSS buffer with 10 µM Fluo-3AM (Fluo-3AM, Shanghai Beyotime Biotech. Co., Ltd., Shanghai, China), and incubated for 30 min at 37 °C in the dark. The cells were then subjected to flow cytometric analysis at 488 nm excitation wavelength [36, 37].

Acknowledgments

This study was supported by the National Natural Science Foundation of China (No. 81173519); the Innovation Team Project Foundation of Beijing University of Chinese Medicine (Lead Compound Discovering and Developing Innovation Team Project Foundation, No. 2011-CXTD-15); Beijing Key Laboratory for Basic and Development Research on Chinese Medicine; and young teachers' scientific research project of Beijing University of Chinese Medicine (No. 2015-JYB JSMS023).

Author Contributions

Ideas and experiment design: Bing Xu, Peng-Long Wang and Hai-Min Lei; Chemistry and Biology: Bing Xu, Wen-Qiang Yan, Xin Xu, Yao-Tian Han; Analysis and interpretation of data: Rui Zhao, Fu-Hao Chu, Gao-Rong Wu; Writing and review of the manuscript: All the authors; Study supervision: Haimin Lei, Penglong Wang.

Conflicts of Interest

The authors declare no conflict of interest.

References

- [1] P.E. Goss, K. Strasser-Weippl, B.L. Lee-Bychkovsky, L. Fan, J. Li, Y. Chavarri-Guerra, P.E.R. Liedke, C.S. Pramesh, T. Badovinac-Crnjevic, Y. Sheikine, Z. Chen, Y. Qiao, Z. Shao, Y. Wu, D. Fan, L.W.C. Chow, J. Wang, Q. Zhang, S. Yu, G. Shen, J. He, A. Purushotham, R. Sullivan, R. Badwe, S.D. Banavali, R. Nair, L. Kumar, P. Parikh, S. Subramanian, P. Chaturvedi, S. Iyer, S.S. Shastri, R. Digumarti, E. Soto-Perez-de-Celis, D. Adilbay, V. Semiglazov, S. Orlov, D. Kaidarova, I. Tsimafeyeu, S. Tatishchev, K.D. Danishevskiy, M. Hurlbert, C. Vail, J.S. Louis, A. Chan, Challenges to effective cancer control in China, India, and Russia, *Lancet Oncol.* 15 (2014) 489-538.
- [2] R.L. Siegel, K.D. Miller, A. Jemal, Cancer statistics, 2015, *CA Cancer J. Clin.* 65 (2015) 5-29.
- [3] A.M. Florea, D. Büsselberg, Cisplatin as an anti-tumor drug: cellular mechanisms of activity, drug resistance and induced side effects, *Cancers* 3 (2011) 1351-1371.
- [4] J.J. Monsuez, J.C. Charniot, N. Vignat, J.Y. Artigou, Cardiac side-effects of cancer chemotherapy, *Int. J. Cardiol.* 144 (2010) 3-15.
- [5] A. Urruticoechea, R. Alemany, J. Balart, A. Villanueva, F. Viñals, G. Capellá, Recent advances in cancer therapy: an overview, *Curr. Pharm. Des.* 16 (2010) 3-10.
- [6] K.S. Chan, C.G. Koh, H.Y. Li, Mitosis-targeted anti-cancer therapies: where they stand, *Cell Death Dis.* 3 (2012) e411.
- [7] M.K. Shanmugam, X. Dai, A.P. Kumar, B.K. Tan, G. Sethi, A. Bishayee, Oleanolic acid and its synthetic derivatives for the prevention and therapy of cancer: preclinical and clinical evidence, *Cancer Lett.* 346 (2014) 206-216.
- [8] L. Fang, M. Wang, S. Gou, X. Liu, H. Zhang, F. Cao, Combination of amino acid/dipeptide with nitric oxide donating oleanolic acid derivatives as PepT1 targeting antitumor prodrugs, *J. Med. Chem.* 57 (2014) 1116-1120.
- [9] K.G. Cheng, C.H. Su, L.D. Yang, J. Liu, Z.F. Chen, Synthesis of oleanolic acid dimers linked at C-28 and evaluation of anti-tumor activity, *Eur. J. Med. Chem.* 89 (2015) 480-489.
- [10] S. Rashid, B.A. Dar, R. Majeed, A. Hamid, B.A. Bhat, Synthesis and biological evaluation of ursolic acid-triazolyl derivatives as potential anti-cancer agents, *Eur. J.*

- 789 Med. Chem. 66 (2013) 238-245.
- 790 [11] H. Chen, G. Li, P. Zhan, X. Guo, Q. Ding, S. Wang, X. Liu, Design, synthesis
791 and biological evaluation of novel ligustrazinylated derivatives as potent
792 cardiovascular agents, Med. Chem. Commun. 4 (2013) 827-832.
- 793 [12] Z. Li, F. Yu, L. Cui, W. Chen, S. Wang, P. Zhan, Y. Shen, X. Liu, Ligustrazine
794 Derivatives. Part 8: Design, Synthesis, and Preliminary Biological Evaluation of
795 Novel Ligustrazinyl Amides as Cardiovascular Agents, Med. Chem. 10 (2014) 81-9.
- 796 [13] C.Y. Chang, T.K. Kao, W.Y. Chen, Y.C. Ou, J.R. Li, S.L. Liao, S.L. Raung, C.J.
797 Chen, Tetramethylpyrazine inhibits neutrophil activation following permanent
798 cerebral ischemia in rats, Biochem. Biophys. Res. Commun. 463 (2015) 421-427.
- 799 [14] J. Pan, J.F. Shang, G.Q. Jiang, Z.X. Yang, Ligustrazine induces apoptosis of
800 breast cancer cells in vitro and in vivo, J. Cancer Res. Ther. 11 (2015) 454.
- 801 [15] J. Han, J. Song, X. Li, M. Zhu, W. Guo, W. Xing, R. Zhao, X. He, X. Liu, S.
802 Wang, Y. Li, H. Huang, X. Xu, Ligustrazine suppresses the growth of HRPC Cells
803 through the inhibition of cap-dependent translation via both the mTOR and the
804 MEK/ERK pathways, Anticancer Agents Med. Chem. 15 (2015) 764-772.
- 805 [16] Y. Ai, B. Zhu, C. Ren, F. Kang, J. Li, Z. Huang, Y. Lai, S. Peng, K. Ding, J. Tian,
806 Y. Zhang, Discovery of New Monocarbonyl Ligustrazine–Curcumin Hybrids for
807 Intervention of Drug-Sensitive and Drug-Resistant Lung Cancer, J. Med. Chem. 59
808 (2016) 1747-1760.
- 809 [17] P. Wang, G. She, Y. Yang, Q. Li, H. Zhang, J. Liu, Y. Cao, X. Xu, H. Lei,
810 Synthesis and biological evaluation of new ligustrazine derivatives as anti-tumor
811 agents, Molecules 17 (2012) 4972-4985.
- 812 [18] P. Wang, Y. Zhang, K. Xu, Q. Li, H. Zhang, J. Guo, D. Pang, Y. Cheng, H. Lei,
813 A new ligustrazine derivative - pharmacokinetic evaluation and antitumor activity by
814 suppression of NF- κ B/p65 and COX-2 expression in S180 mice, Pharmazie 68 (2013)
815 782-789.
- 816 [19] B. Xu, F. Chu, Y. Zhang, X. Wang, Q. Li, W. Liu, X. Xu, Y. Xing, J. Chen, P.
817 Wang, H. Lei, A series of new ligustrazine-triterpenes derivatives as anti-tumor
818 agents: design, synthesis, and biological evaluation, Int. J. Mol. Sci. 16 (2015)

- 819 21035-21055.
- 820 [20] P. Wang, Y. Cheng, K. Xu, Y. An, W. Wang, Q. Li, Q. Han, Q. Li, H. Zhang, H.
821 Lei, Synthesis and antitumor evaluation of one novel tetramethylpyrazine-rhein
822 derivative, *Asian J. Chem.* 25 (2013) 4885.
- 823 [21] F. Chu, X. Xu, G. Li, H. Gu, K. Xu, Y. Gong, B. Xu, M. Wang, H. Zhang, Y.
824 Zhang, P. Wang, H. Lei, Amino acid derivatives of ligustrazine-oleanolic acid as new
825 cytotoxic agents, *Molecules* 19 (2014) 18215-18231.
- 826 [22] K. Xu, X. Xu, F. Chu, M. Wang, P. Wang, G. Li, J. Song, Y. Zhang, H. Lei,
827 Synthesis and biological evaluation of T-OA analogues as the cytotoxic agents, *Res.*
828 *Chem. Intermediat.* 41 (2015) 6257-6269.
- 829 [23] S. Schwarz, B. Siewert, N.M. Xavier, A.R. Jesus, A.P. Rauter, R. Csuk, A
830 “natural” approach: synthesis and cytotoxicity of monodesmosidic glycyrrhetinic acid
831 glycosides, *Eur. J. Med. Chem.* 72 (2014) 78-83.
- 832 [24] S. Schwarz, R. Csuk, Synthesis and antitumour activity of glycyrrhetinic acid
833 derivatives, *Bioorg. Med. Chem.* 18 (2010) 7458-7474.
- 834 [25] R. Csuk, S. Schwarz, B. Siewert, R. Kluge, D. Ströhl, Synthesis and cytotoxic
835 activity of methyl glycyrrhetinate esterified with amino acids, *Zeitschrift für*
836 *Naturforschung B* 67 (2012) 731-746.
- 837 [26] L. Deng, X. Guo, L. Zhai, Y. Song, H. Chen, P. Zhan, J. Wu, X. Liu,
838 Ligustrazine Derivatives. Part 4: Design, Synthesis, and Biological Evaluation of
839 Novel Ligustrazine-based Stilbene Derivatives as Potential Cardiovascular Agents,
840 *Chem. Biol. Drug Des.* 79 (2012) 731-739.
- 841 [27] A.L. Hopkins, C.R. Groom, A. Alex, Ligand efficiency: a useful metric for lead
842 selection, *Drug Discov. Today* 9 (2004) 430-431.
- 843 [28] T. Wunberg, M. Hendrix, A. Hillisch, M. Lobell, H. Meier, C. Schmeck, H. Wild,
844 B. Hinzen, Improving the hit-to-lead process: data-driven assessment of drug-like and
845 lead-like screening hits, *Drug Discov. Today* 11 (2006) 175-180.
- 846 [29] N.A. Meanwell, Improving drug candidates by design: a focus on
847 physicochemical properties as a means of improving compound disposition and safety,
848 *Chem. Res. Toxicol.* 24 (2011) 1420-1456.

- 849 [30] C.E.C.A. Hop, Role of ADME studies in selecting drug candidates: Dependence
850 of ADME parameters on physicochemical properties, *Encyclopedia of Drug*
851 *Metabolism and Interactions* 2012.
- 852 [31] P.J. Eddershaw, A.P. Beresford, M.K. Bayliss, ADME/PK as part of a rational
853 approach to drug discovery, *Drug Discov. Today* 5 (2000) 409-414.
- 854 [32] F. Qi, A. Li, L. Zhao, H. Xu, Y. Inagaki, D. Wang, X. Cui, B. Gao, N. Kokudo,
855 M. Nakata, W. Tang, Cinobufacini, an aqueous extract from *Bufo bufo gargarizans*
856 Cantor, induces apoptosis through a mitochondria-mediated pathway in human
857 hepatocellular carcinoma cells, *J. Ethnopharmacol.* 128 (2010) 654-661.
- 858 [33] X. Chen, J. Wang, Q. Qin, Y. Jiang, G. Yang, K. Rao, Q. Wang, W. Xiong, J.
859 Yuan, Mono-2-ethylhexyl phthalate induced loss of mitochondrial membrane
860 potential and activation of Caspase3 in HepG2 cells, *Environ. Toxicol. Pharmacol.* 33
861 (2012) 421-430.
- 862 [34] B.A. Wani, D. Ramamoorthy, M.A. Rather, N. Arumugam, A.K. Qazi, R.
863 Majeed, A. Hamid, S.A. Ganie, B.A. Ganai, R. Anand, A.P. Gupta, Induction of
864 apoptosis in human pancreatic MiaPaCa-2 cells through the loss of mitochondrial
865 membrane potential ($\Delta\Psi$ m) by *Gentiana kurroo* root extract and LC-ESI-MS analysis
866 of its principal constituents, *Phytomedicine* 20 (2013) 723-733.
- 867 [35] D. Bano, P. Nicotera, Ca^{2+} signals and neuronal death in brain ischemia, *Stroke*
868 38 (2007) 674-676.
- 869 [36] M. Wang, Y. Ruan, Q. Chen, S. Li, Q. Wang, J. Cai, Curcumin induced HepG2
870 cell apoptosis-associated mitochondrial membrane potential and intracellular free Ca^{2+}
871 concentration, *Eur. J. Pharmacol.* 650 (2011) 41-47.
- 872 [37] Z. Liu, L. Gong, X. Li, L. YE, B. Wang, J. Liu, J. Qiu, H. Jiao, W. Zhang, J.
873 Chen, J. Wang, Infrasound increases intracellular calcium concentration and induces
874 apoptosis in hippocampi of adult rats, *Mol. Med. Rep.* 5 (2012) 73-77.
- 875 [38] C. Sakalar, M. Yuruk, T. Kaya, M. Aytekin, S. Kuk, H. Canatan, Pronounced
876 transcriptional regulation of apoptotic and TNF–NF-kappa-B signaling genes during
877 the course of thymoquinone mediated apoptosis in HeLa cells, *Mol. Cell. Biochem.*
878 383 (2013) 243-251.

[39] J.R. Nakkala, R. Mata, A.K. Gupta, S.R. Sadras, Biological activities of green silver nanoparticles synthesized with *Acorous calamus* rhizome extract, *Eur. J. Med. Chem.* 85 (2014) 784-794.

[40] L. Costa, R.O. Pinheiro, P.M. Dutra, R.F. Santos, E.F. Cunha-Júnior, E.C. Torres-Santos, A.J. da Silva, P.R. Costa, S.A. Da-Silva, Pterocarpanquinone LQB-118 induces apoptosis in *leishmania (Viannia) braziliensis* and controls lesions in infected hamsters, *PloS one* 9 (2014) e109672.

903 **Captions to the Tables, Fig.s and Schemes.**

904 **Table1** The structures of **TBA** amino acids derivatives **BA-02---BA-15**.

905 **Table 2** The structures of **TBA** dipeptides derivatives **BA-16---BA-27**.

906 **Table 3** The IC₅₀ values of **TBA** amine acids or dipeptide derivatives **BA-X** for
907 different tumor cells and MDCK cells.

908 **Fig. 1.** Morphological detection of apoptosis using Giemsa staining (200×): (a)
909 Control group; (b) 1.5 μM; (c) 3 μM; and (d) 6 μM. The cell morphology was
910 observed under the light microscope after Giemsa staining. The most representative
911 fields are shown. Arrows indicate the typical apoptotic cell.

912 **Fig. 2.** Morphological detection of apoptosis using DAPI staining (200×): (a) control
913 group; (b) 1.5 μM; (c) 3 μM; and (d) 6 μM. The cell morphology was observed under
914 the fluorescence microscope after DAPI staining. The most representative fields are
915 shown. Arrows indicate the typical apoptotic cell.

916 **Fig. 3.** Detection of apoptosis using Annexin V-FITC/PI staining: (a) control group;
917 (b) 2 μM; (c) 3 μM; and (d) 4 μM.

918 **Fig. 4.** Effect of **BA-25** on mitochondrial membrane potential: (a) control group; (b) 2
919 μM; (c) 3 μM; and (d) 4 μM. Cells were determined by flow-cytometric analysis
920 stained with Rhodamine 123 for 30 min. Results are expressed as mean fluorescent
921 intensity (MFI).

922 **Fig. 5.** Effect of **BA-25** on intracellular free Ca²⁺ in HepG2 cells: (a) control group; (b)
923 2 μM; (c) 3 μM; and (d) 4 μM. After being treated with 2.0, 3.0 and 4.0 μM **BA-25**
924 for 72 h, cells were determined by flow-cytometric analysis stained with Fluo-3AM
925 for 30 min. Results are expressed as mean fluorescent intensity (MFI).

926 **Scheme 1.** Synthesis of the intermediate 2-(chloromethyl)-3,5,6-trimethylpyrazine (**5**).

927 *Reagents and Conditions:* (a) aceticacid (AcOH), 30% H₂O₂, reflux, 90°C, 6h; (b)

acetic anhydride (Ac_2O), reflux, 105°C , 2h; (c) THF: MeOH: H_2O =3:1:1, NaOH, 1h;
(d) THF, TsCl, TEA, DMAP, 12h.

Scheme 2. Synthesis of the derivative **TBA (BA-01)**. *Reagents and Conditions:* (a) dry DMF, dry K_2CO_3 , 25°C , 12h.

Scheme 3. Synthesis of the **TBA** amino acids derivatives **BA-02---BA-15**. *Reagents and Conditions:* Boc-amino acids or Cbz-amino acids, DCM, DMAP, EDCI, 25°C , 12h; (b) TFA in dry DCM, 0°C , 2h or Pd/C (10%), MeOH, 25°C , 12h; (c) TBDMSCl, Imidazole, DMF, 25°C , 12h; (d) TBAF, THF, 25°C , 1.5h.

Scheme 4. Synthesis of the **TBA** dipeptide derivatives **BA-16---BA-27**. *Reagents and Conditions:* (a) Boc-amino acids, HOBt, EDCI, DIPEA, 25°C , 12h; (b) TFA in dry DCM, 0°C , 2h.

950 **Table1** The structures of **TBA** amino acids derivatives **BA-02---BA-15**

Compound	R	Compound	R
BA-02	L-Gly	BA-09	L-Pyr
BA-03	L-Phe	BA-10	L-Lys
BA-04	L-Ala	BA-11	L-Trp
BA-05	L-Asp	BA-12	L-Sar
BA-06	L-Pro	BA-13	L-Val
BA-07	L-Leu	BA-14	L-Thr
BA-08	L-Ile	BA-15	L-Ser

951 **Table 2** The structures of **TBA** dipeptides derivatives **BA-16---BA-27**

compound	R ₁	R ₂
BA-16	L-Gly	L-Gly
BA-17	L-Sar	L-Sar
BA-18	L-Sar	L-Pro
BA-19	L-Gly	L-Ala
BA-20	L-Gly	L-Pro
BA-21	L-Gly	L-Sar
BA-22	L-Ala	L-Ala
BA-23	L-Ala	L-Gly
BA-24	L-Ala	L-Pro
BA-25	L-Ala	L-Sar
BA-26	L-Sar	L-Gly
BA-27	L-Sar	L-Ala

952 **Table 3** The IC₅₀ values of **TBA** amine acids or dipeptide derivatives **BA-X** for
 953 different tumor cells and MDCK cells

Compd	IC ₅₀ (μM)					
	HepG2	HT-29	Hela	BGC-823	A549	MDCK
BA-01	5.70±1.77	7.41±2.34	8.00±1.89	6.87±0.21	3.56±0.31	18.20±0.18

BA-02	6.77±0.67	3.97±0.59	4.24±0.70	3.87±0.22	3.62±0.31	5.82±0.50
BA-03	>40	>20	>40	>20	>40	>40
BA-04	>20	7.74±0.14	6.62±1.41	6.16±0.58	6.33±0.17	>40
BA-05	>20	>20	>20	>20	>20	>40
BA-06	4.54±0.46	2.73±0.35	6.33±0.02	3.47±0.2	3.36±0.48	10.15±4.05
BA-07	>40	>20	>20	>20	>20	>40
BA-08	12.73±0.8	15.89±2.9	>20	>20	14.52±5.3	>40
BA-09	5.86±0.45	3.78±0.89	6.59±0.34	4.70±0.42	4.11±0.56	9.24±0.21
BA-10	2.39±0.70	2.64±0.5	2.62±0.36	2.16±1.10	1.26±0.83	>40
BA-11	>40	7.41±2.34	>20	>20	>20	>40
BA-12	4.5±0.65	1.10±0.67	3.96±1.08	3.97±2.15	3.05±0.34	9.08±0.22
BA-13	5.91±0.05	>20	8.63±0.75	7.14±1.70	6.90±0.37	>40
BA-14	3.64±0.49	6.66±0.92	8.39±0.58	7.05±0.53	4.18±0.81	>40
BA-15	4.03±0.22	4.35±1.31	2.74±0.97	6.21±0.29	4.39±2.76	8.56±1.19
BA-16	4.0±0.87	3.19±0.4	2.40±0.04	2.88±0.42	1.95±0.58	7.45±1.15
BA-17	3.94±0.02	8.32±1.07	5.08±1.61	4.10±0.13	4.83±0.01	10.91±1.4
BA-18	3.75±0.36	5.98±0.29	3.02±0.12	1.83±1.07	3.91±1.13	11.28±0.21
BA-19	2.27±0.67	3.67±0.42	3.19±0.97	4.99±0.33	3.25±0.15	16.23±5.90
BA-20	3.48±1.13	4.11±1.05	2.20±0.43	0.84±0.39	2.98±1.61	6.63±0.41
BA-21	5.27±1.29	3.37±2.59	7.38±0.38	2.07±0.99	3.02±1.08	20.64±5.89
BA-22	1.93±0.49	4.18±1.20	4.49±0.82	2.51±1.68	2.54±0.44	10.21±1.14
BA-23	2.17±0.26	4.38±2.39	5.57±0.55	1.49±0.63	2.45±0.80	>40
BA-24	3.39±1.01	3.56±0.07	2.33±0.46	2.52±0.16	4.08±0.45	>40
BA-25	3.09±1.49	1.70±0.34	1.74±0.99	1.79±0.28	3.25±1.10	10.84±0.27
BA-26	4.94±0.04	3.31±0.28	2.62±1.13	3.43±0.42	2.96±0.76	8.08±0.13
BA-27	4.27±0.25	3.86±1.33	4.55±1.49	4.38±0.57	5.18±1.33	14.56±1.88
DPP	3.42±0.68	4.1±1.17	5.60±0.78	4.25±0.32	3.85±0.63	12.38±1.23

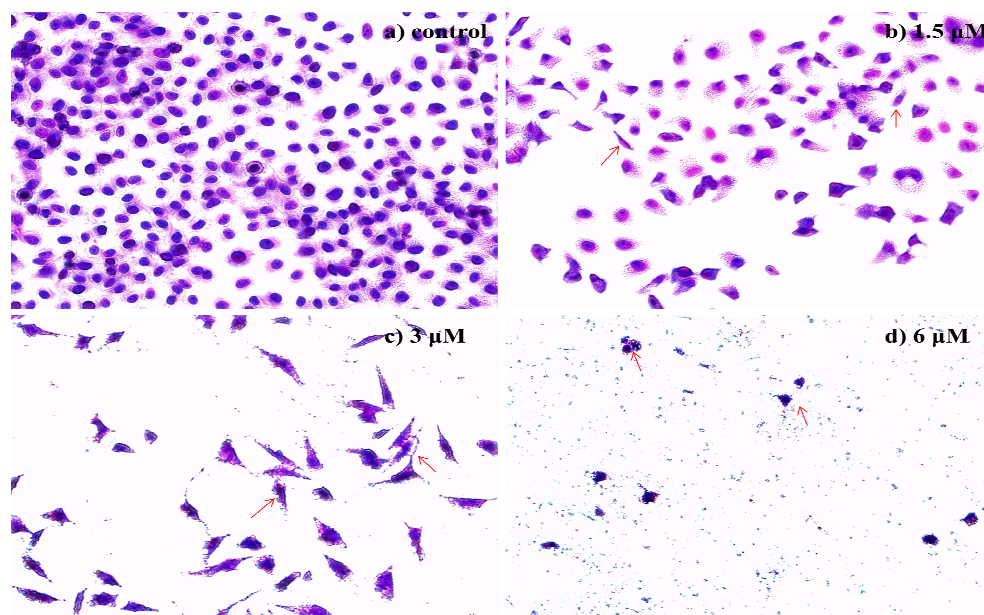


Fig. 1. Morphological detection of apoptosis using Giemsa staining (200 \times).

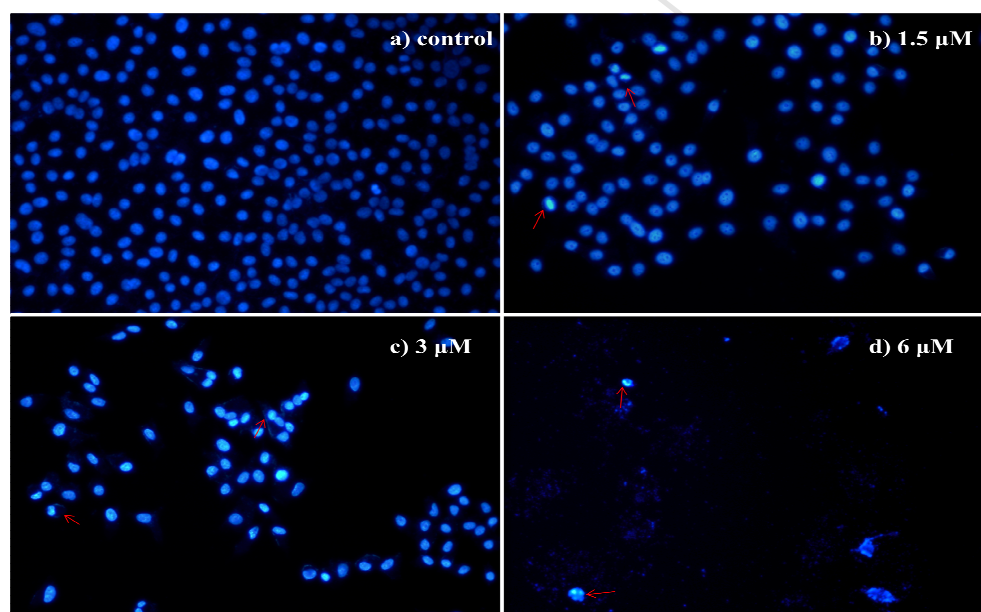


Fig. 2. Morphological detection of apoptosis using DAPI staining (200 \times).

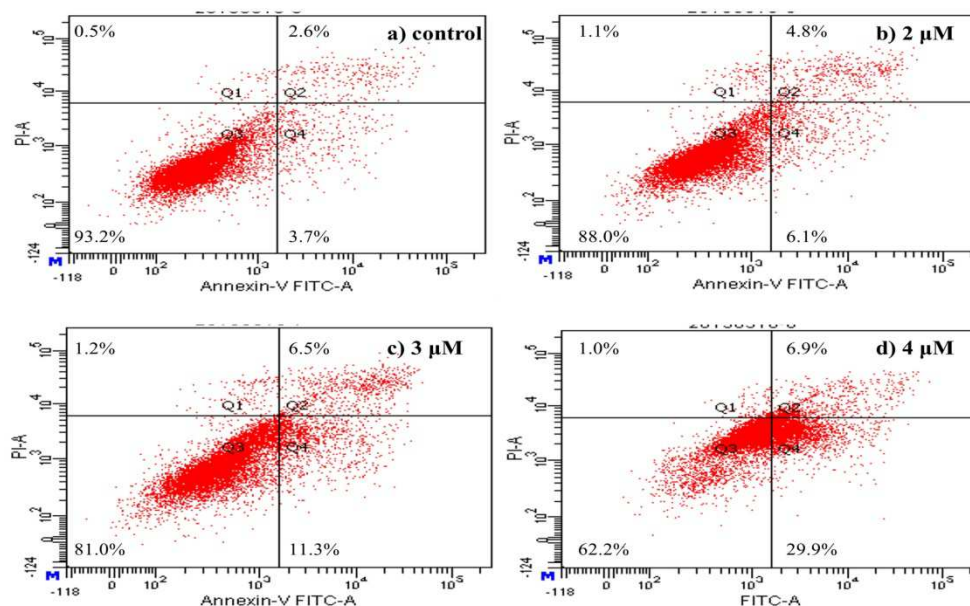


Fig. 3. Detection of apoptosis using Annexin V-FITC/PI staining.

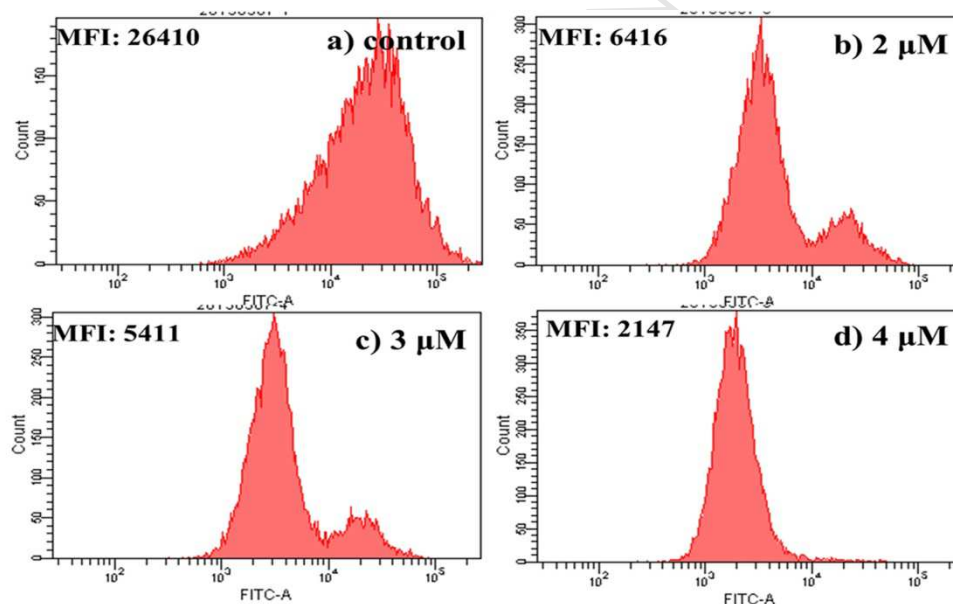


Fig. 4. Effect of **BA-25** on mitochondrial membrane potential.

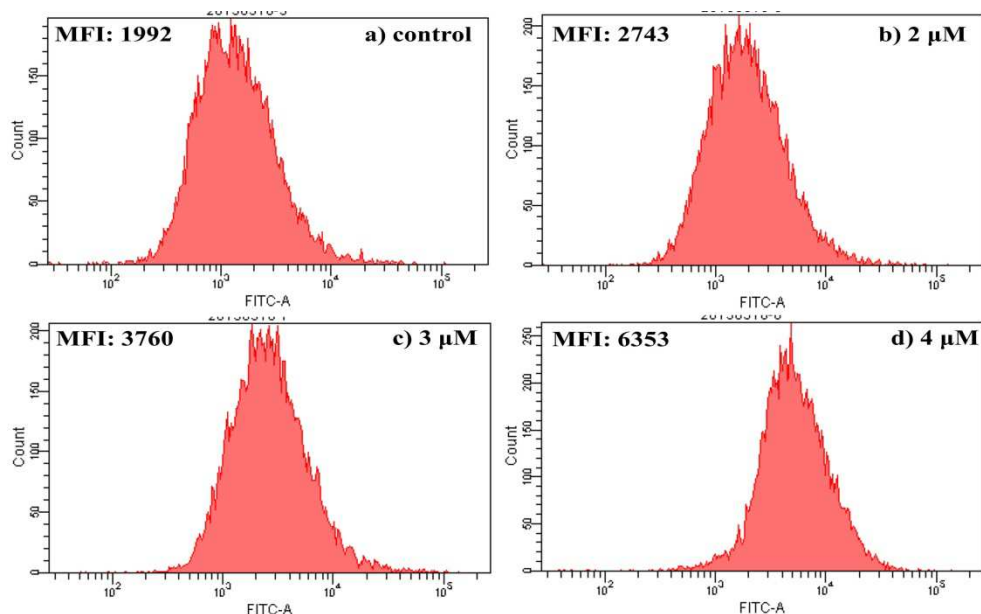
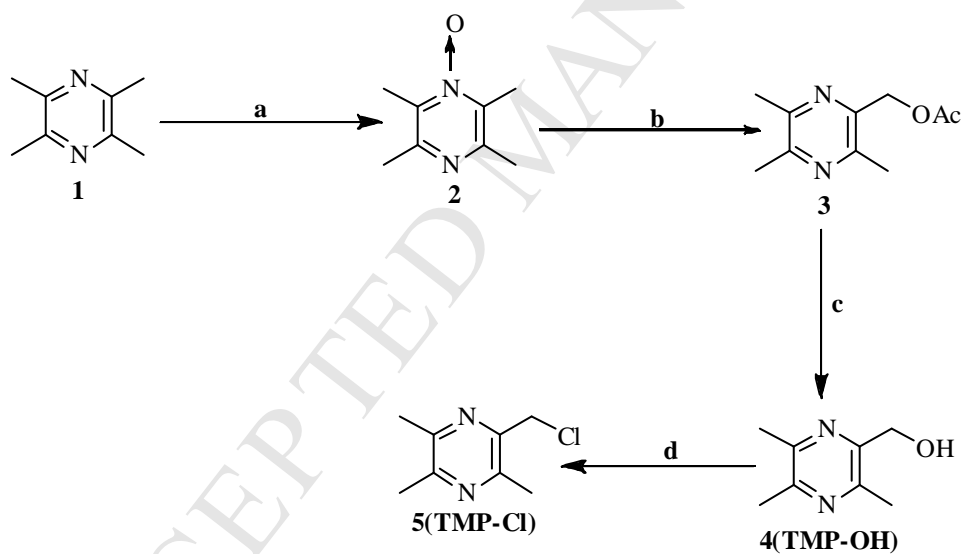
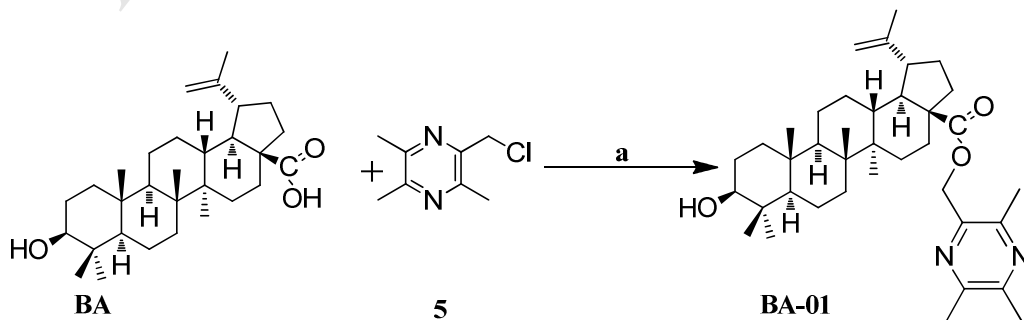


Fig. 5. Effect of **BA-25** on intracellular free Ca^{2+} in HepG2 cells.



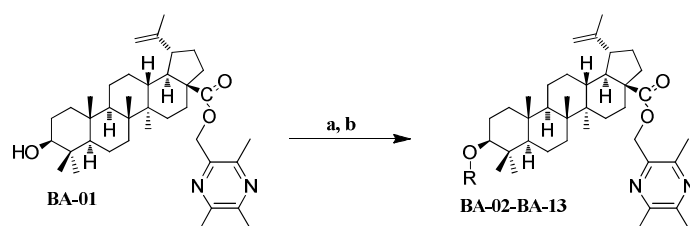
Scheme 1. Synthesis of the intermediate 2-(chloromethyl)-3,5,6-trimethylpyrazine (5).



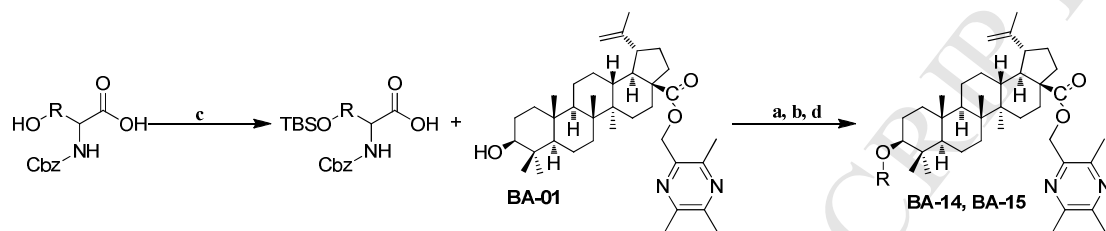
981

Scheme 2. Synthesis of the derivative TBA (BA-01).

982



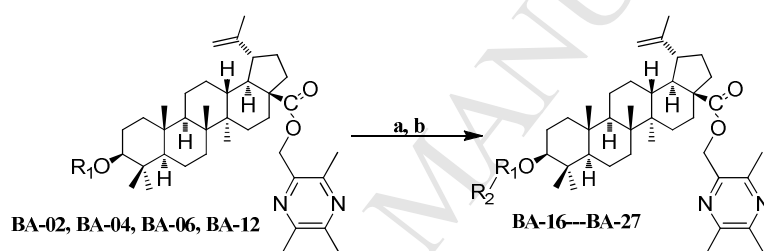
983



984

Scheme 3. Synthesis of the TBA amino acids derivatives BA-02---BA-15.

985



986

Scheme 4. Synthesis of the TBA dipeptide derivatives BA-16---BA-27.

Highlights

- a. Twenty-six **TBA** amino acid/dipeptide derivatives were synthesized.
- b. **TBA** amino acid/dipeptide derivatives showed potent cytotoxicity on tumor cell, and low toxicity on normal cell.
- c. **BA-25**-induced apoptosis was associated with loss of mitochondrial membrane potential.
- d. **BA-25**-induced apoptosis was associated with increase of intracellular free Ca^{2+} concentration.